



## FORMULATION, OPTIMIZATION AND EVALUATION OF IMATINIB MESYLATENANOPARTICLES

K. Lakshmikanth<sup>1\*</sup>, MD Iftekhhar Ahmed khan<sup>2</sup>, Shaik Neha Samreen<sup>3</sup>, M. Priyanka<sup>4</sup>, B Sandhya Rani<sup>5</sup>, MISBA<sup>6</sup>, Dr. Md Sultan Ali Basha<sup>7</sup>

<sup>1,3,4</sup>Research scholar Department of Pharmaceutics, Safa College of Pharmacy, Kurnool

<sup>2</sup>Associate Professor, Department of Pharmaceutics, Safa College of Pharmacy, Kurnool

<sup>5,6</sup>Assistant Professor, Safa College of Pharmacy, Kurnool

<sup>7</sup>Professor and Principal, Safa College of Pharmacy, Kurnool

**\*Corresponding Author:-K. Lakshmikanth**

\*Department of Pharmaceutics, Safa College of Pharmacy, Kurnool Email  
id: lucky84kanth@gmail.com

### ABSTRACT

The objective of this study was to develop, optimize, and evaluate Imatinib mesylate nanoparticles using a Box-Behnken Design of Experiment (DoE). The independent factors considered were the drug-to-polymer ratio, stabilizer concentration, and stirring speed, while the dependent factors were entrapment efficiency and drug release characteristics. Imatinib mesylate nanoparticles were prepared through the solvent evaporation method using Ethyl cellulose as the polymer and PVA as the stabilizer. The prepared nanoparticles underwent characterization for percentage yield, drug content, entrapment efficiency, particle size, zeta potential, polydispersity index, FTIR, DSC, SEM, and in-vitro drug release profiles. Evaluation results demonstrated promising entrapment efficiency, favourable zeta potential, optimal particle size, and prolonged drug release. FTIR and DSC studies indicated no interaction between the drug and excipients. The optimized formulation exhibited high entrapment efficiency (99.3%) and sustained drug release (97.42%) for a 24-hour duration, following zero-order release kinetics and a non-Fickian diffusion mechanism. These findings suggest that Imatinib mesylate nanoparticles hold potential as effective drug delivery systems for the treatment of chronic myeloid leukemia.

**Keywords:** Imatinib mesylate, Ethyl cellulose, Box-Behnken Design, zero-order release kinetics.

### INTRODUCTION

Chronic myeloid leukemia (CML) is a hematopoietic stem cell disorder characterized by the abnormal proliferation of myeloid cells in the bone marrow and blood. It is primarily caused by the reciprocal translocation between chromosomes 9 and 22, resulting in the formation of the Philadelphia chromosome and the BCR-ABL fusion gene [1]. This fusion gene encodes a constitutively active tyrosine kinase, leading to uncontrolled cell growth, impaired differentiation, and increased resistance to apoptosis [2]. Imatinib mesylate (IM) is a tyrosine kinase inhibitor that specifically targets BCR-ABL and has revolutionized the treatment of CML. It binds to the ATP-binding site of the BCR-ABL protein, inhibiting its tyrosine kinase activity and thereby suppressing the proliferation of leukemic cells [3]. However, conventional IM formulations face challenges such as poor solubility, low oral bioavailability, and rapid metabolism, which can limit its therapeutic efficacy [4]. To overcome these

limitations, the development of drug delivery systems that can enhance the solubility, bioavailability, and sustained release of IM is crucial. Nanoparticles have emerged as promising carriers for drug delivery due to their unique properties, including high surface area, stability, and the ability to protect drugs from enzymatic degradation [5]. Several nanoparticle-based formulations have been investigated for IM delivery, including polymeric nanoparticles, liposomes, and solid lipid nanoparticles [6, 7]. However, there is still a need to optimize these formulations for improved drug loading, controlled release, and enhanced therapeutic efficacy. In this study, we aimed to formulate, optimize, and evaluate IM nanoparticles prepared using the solvent evaporation method. Ethyl cellulose (EC) was selected as the polymeric matrix due to its biocompatibility, ease of processing, and controlled release properties. Polyvinyl alcohol (PVA), a commonly used stabilizer, was employed to prevent particle aggregation and ensure stability during formulation. We employed the Box-Behnken Design of Experiment (DoE) to systematically investigate the effects of key formulation parameters, including the drug-to-polymer ratio, stabilizer concentration, and stirring speed, on the entrapment efficiency and drug release characteristics of IM nanoparticles. The entrapment efficiency of nanoparticles is an important parameter that reflects the percentage of drug encapsulated within the particles, indicating the effectiveness of the formulation in drug loading [8]. Additionally, the particle size of nanoparticles has a significant impact on their cellular uptake, biodistribution, and stability, influencing their therapeutic performance [9]. The zeta potential of nanoparticles, which represents their surface charge, can affect their colloidal stability and interaction with biological components [10]. Therefore, these parameters were considered critical in designing an effective IM nanoparticle formulation. Furthermore, understanding the drug release behaviour from nanoparticles is crucial for controlled and sustained drug delivery. Different release mechanisms, such as zero-order and Fickian diffusion, can be investigated to identify the release kinetics and the dominant mechanism of drug release from the nanoparticles [11]. Moreover, the compatibility between the drug and excipients used in the formulation is essential to ensure that there are no chemical interactions that may impact drug stability or efficacy. Therefore, Fourier-transform infrared spectroscopy (FTIR) and differential scanning calorimetry (DSC) analyses were performed to investigate the possible drug-excipient interactions [12]. The objectives of this study were to optimize IM nanoparticle formulation using the Box-Behnken DoE, evaluate the physicochemical properties of the nanoparticles, assess their in vitro drug release behaviour, and investigate the potential of these nanoparticles as effective drug delivery vehicles for the treatment of CML. By optimizing the formulation parameters and understanding the release kinetics, this research aims to contribute to the design of more efficient and patient-friendly IM formulations.

## **MATERIAL AND METHODS**

### **Preformulation studies**

Preformulation testing is the initial step in the rational development of any dosage forms. The main importance of preformulation is to maximize the chances of formulating an acceptable, safe, and stable product.

#### **Characterization of Imatinib mesylate**

**Description:** The physical characteristics of the pure drug were visually evaluated.

**Solubility studies:** Solubility studies of Imatinib mesylate were done by dissolving 10 mg of pure drug in 10 ml of phosphate buffer pH 6.8.

**Melting point:** The crystalline substance was powdered and filled in a capillary tube. The tube was then placed in a melting point apparatus to determine the temperature required for the substance to melt. The melting point of Imatinib mesylate was noted.

#### **Drug excipient compatibility studies**

There is a possibility of drug-excipient interaction in any formulation due to their intimate contact. It is necessary to determine the possible interaction between excipients used in the formulation. The drug interacting with one or more excipients were subjected to analysis using FTIR & DSC.

**FTIR studies:**

Fourier transform infrared spectroscopy (FTIR) was used to find any possible incompatibilities between the drug and excipients. The spectrum was recorded for Imatinib mesylate and other excipients used in the formulations using an infrared spectrophotometer. The samples were blended with KBr and compressed to form a KBr pellet. The pellet was placed in the light path and the spectrum was recorded. The characteristic peaks of the functional groups were interpreted.

**DSC studies:**

Differential scanning calorimetry (DSC) was used to analyze the difference in heat required to increase the temperature of a sample and reference. The samples were subjected to DSC studies using a DSC equipment. The samples were sealed in aluminum pans and scanned at a specific rate with a nitrogen purge. The heat capacity and temperature data were collected.

**Determination of  $\lambda_{\text{max}}$  for Imatinib mesylate**

Concentrations of 100  $\mu\text{g/ml}$  were prepared by dissolving 100 mg of the drug in 100 ml of phosphate buffer pH 6.8. From this solution, a secondary solution with a concentration of 10  $\mu\text{g/ml}$  was prepared. The solution was scanned between the wavelengths of 400 to 200 nm to determine the wavelength at which maximum absorbance was observed.

**Calibration curve of Imatinib mesylate**

A stock solution of Imatinib mesylate was prepared with a concentration of 1000  $\mu\text{g/ml}$ . From this stock solution, a series of solutions with concentrations ranging from 2 to 10  $\mu\text{g/ml}$  were prepared. The absorbance of the solutions was measured at 255 nm using a UV-visible spectrophotometer. A calibration curve was plotted using the absorbance values.

**Preparation of phosphate buffer pH 6.8:**

A 0.2M potassium dihydrogen phosphate solution was prepared by dissolving 27.218 g of potassium dihydrogen phosphate in water and diluting to 1000 ml. A 0.2M NaOH solution was prepared by dissolving sodium hydroxide in water [13].

**Formulation, Optimization, and Evaluation of Imatinib Mesylate Nanoparticles**

The formulation was designed using a Box-Behnken design. Three formulation variables - drug: polymer ratio, concentration of PVA, and stirring speed - were evaluated at two levels. Experimental trials were performed at all 17 possible combinations, including 4 replicate points. In vitro drug release and entrapment efficiency were selected as dependent variables. The design and formulation variables were summarized in tables.

**Table 2.** Design summary of formulation variables.

Factor	Name	Units	Type	Minimum	Maximum	Coded Low	Coded High
A	Polymer	ratio	Numeric	1.000	10.00	-1 $\leftrightarrow$ 1.00	+1 $\leftrightarrow$ 10.0
B	PVA	%	Numeric	0.4	1.5	-1 $\leftrightarrow$ 0.4	+1.0 $\leftrightarrow$ 1.5
C	Stirring speed(rpm)	-	Numeric	1000	3000	-1 $\leftrightarrow$ 1000	+1 $\leftrightarrow$ 3000

**Preparation of Imatinib mesylate Nanoparticles**

Imatinib mesylate nanoparticles were prepared using the solvent evaporation technique. Imatinib mesylate and the polymer ethyl cellulose were dissolved in a mixture of organic solvents. The drug-polymer solution was injected into an aqueous PVA solution and stirred. The obtained suspension was filtered and dried to obtain Imatinib mesylate nanoparticles.

**Table 2. Formulation table obtained from Box-Behnken Design**

S.no	Formulation Code	Std	Run	Drug: polymer ratio	Concentration stabilizer (%)	Stirring speed (rpm)
1.	INP1	7	1	1	0.95	3000
2.	INP2	5	2	1	0.95	1000
3.	INP3	1	3	1	0.4	2000
4	INP4	11	4	5.5	0.4	3000
5.	INP5	10	5	5.5	1.5	1000
6.	INP6	13	6	5.5	0.95	2000
7.	INP7	14	7	5.5	0.95	2000
8.	INP8	8	8	10	0.95	3000
9.	INP9	4	9	10	1.5	2000
10.	INP10	3	10	1	1.5	2000
11.	INP11	17	11	5.5	1.5	2000
12.	INP12	15	12	5.5	0.95	2000
13.	INP13	6	13	10	0.95	1000
14.	INP14	2	14	10	0.4	2000
15.	INP15	12	15	5.5	1.5	3000
16.	INP16	9	16	5.5	0.4	1000
17.	INP17	16	17	5.5	0.95	2000

### Evaluation Parameters

Several evaluation parameters were used to assess the quality of the Imatinib mesylate nanoparticles. These parameters included percentage yield, determination of drug content, entrapment efficiency, particle size, zeta potential, polydispersity index, surface morphology by SEM, in-vitro drug release studies, and drug release kinetics. The specific methodologies for each parameter were described [14-15].

### Regression Model

Regression analysis was used to optimize the formulation based on the in vitro release study. Linear or first-order regression models, quadratic models, and nonlinear regression models were used to analyze the data. The best-fit model was selected based on statistical parameters such as the coefficient of determination and ANOVA results.

### Analysis of Formulation Variables by Design Expert

The values of response variables were entered into Design Expert software for analysis. The software generated diagnostic and model graphs, including perturbation, interaction, contour, and 3D surface graphs. The best-fit model was selected based on statistical parameters and analysis of variance [16].

## RESULTS

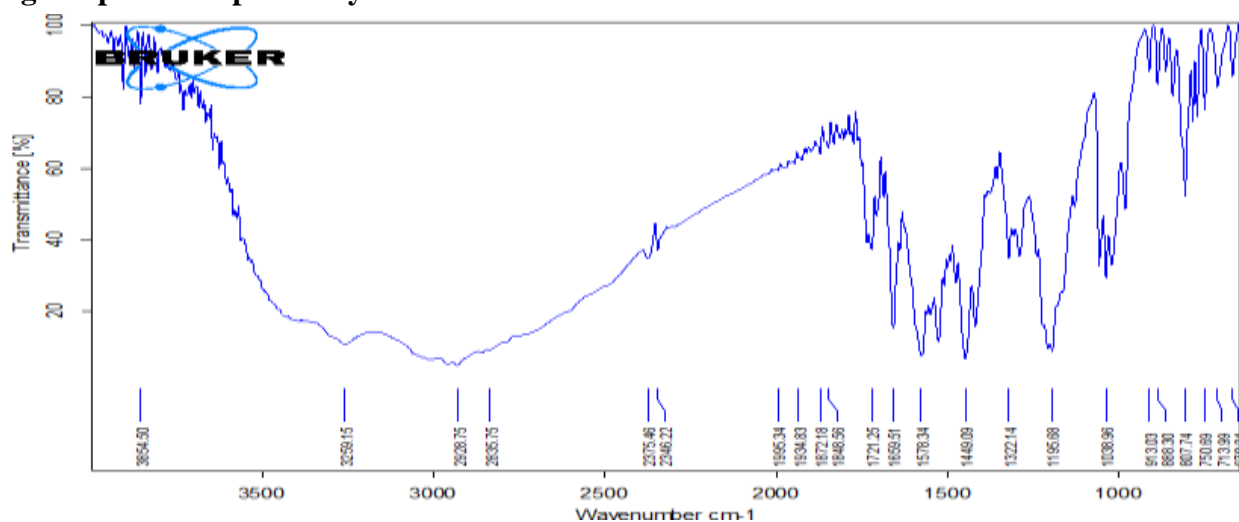
### Preformulation study: Characterization of imatinib mesylate

**Table 3.** Characterization of pure drug

S.NO	CHARACTER	SPECIFICATION	OBSERVATION
1	Description	White to off-white to brownish or yellowish powder	<b>Yellow powder</b>
2	Solubility	Soluble in all pH (1-7.5), but it is insoluble in n-octanol, acetone and acetonitrile	<b>Soluble in pH 6.8 phosphate buffer 0.5 mg/ml.</b>
3	Melting point	<b>225-230°C</b>	<b>226.5°C</b>

As per the procedure the solubility and melting point were performed and the results as per the specification & were reported in the table 3.

### Drug excipient compatibility studies:

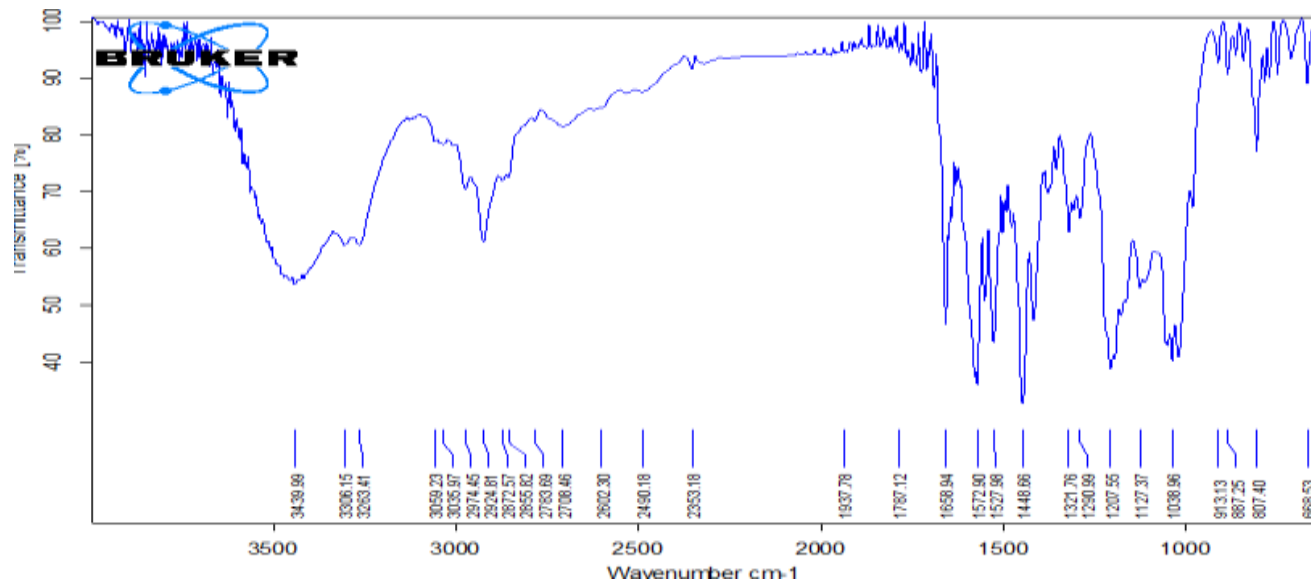


**Fig. 1.** FTIR spectrum of Imatinib mesylate

**Table 4:** Characteristic peaks observed for Imatinib mesylate.

S.NO	Type of Bond	Actual frequency( $\text{cm}^{-1}$ )	Observed frequency( $\text{cm}^{-1}$ )	Conformation group
1.	CH stretching	2800-2900	2928.75	Methyl
2.	NH stretching	3300-3500	3259.15	Amide
3..	C=O stretching	1700-1730	1721.25	Ketone
4.	C=C stretching	1475-1600	1449.09	Aromatic C=C
5.	C-H stretching ( $\text{CH}_3$ )	2800-2950	2835.75	Aromatic C-H

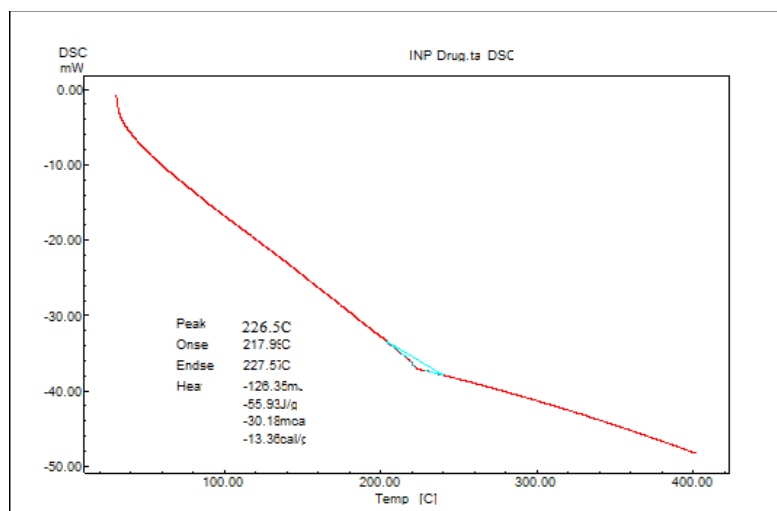
The characteristic peaks obtained from FTIR spectrum confirms the drug is Imatinib mesylate.

**Fig 2. FTIR Spectrum of Imatinib mesylate and ethyl cellulose****Table 5: Characteristic peaks observed for Imatinib mesylate +ethyl cellulose.**

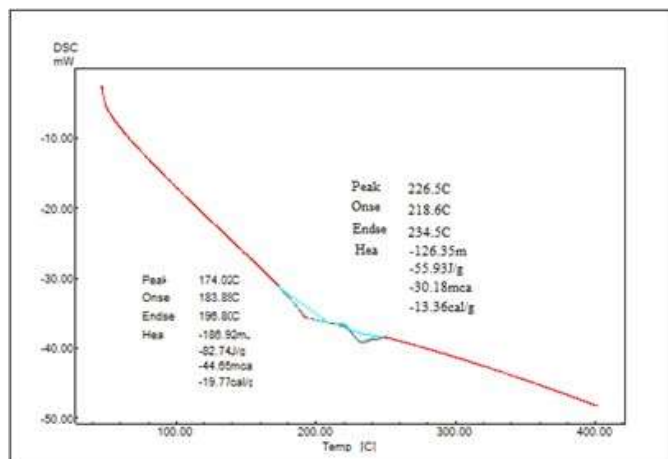
S.NO	Type of Bond	Actual frequency( $\text{cm}^{-1}$ )	Observed frequency ( $\text{cm}^{-1}$ )	Conformation
1.	CH stretching	2800-2900	2855.82	Methyl
2.	NH stretching	3300-3500	3263.41	Amide
3.	C=O stretching	1745-1775	1781.12	Ketone
4.	C=C stretching	1475-1600	1572.90	Aromatic C=C
5.	C-H stretching ( $\text{CH}_3$ )	2800-2950	2872.57	Aromatic C-H
6.	OH stretching	2400-3400	3306.15	Hydroxyl

The FTIR spectra of **Fig. 2** has all the characteristic peaks of drug indicating the ethyl cellulose is compatible with ethyl cellulose.

## DSC STUDIES

**Fig 3. DSC of Pure Drug**

### DSC of Physical mixture



DSC study of pure drug Imatinib mesylate was performed and shown in above figure 3. The study starts from zero and extended up to 400<sup>o</sup> C. The peak onset at 217.9 <sup>o</sup> C and end set at 227.5 <sup>o</sup> C, in which the peak is observed at 226.5 <sup>o</sup> C indicating that the drug's melting point and its identification as Imatinib mesylate. DSC study of drug and polymer physical mixture was performed and shown in above figure 4. The study starts from zero and extended up to 400<sup>o</sup> C. Two peaks were observed in DSC spectrum at 174.02<sup>o</sup>C and 226.5 <sup>o</sup>C indicating ethyl cellulose and Imatinib mesylate are compatible with each other.

### Determination of $\lambda_{max}$ of Imatinib mesylate in pH 6.8 phosphate buffer.

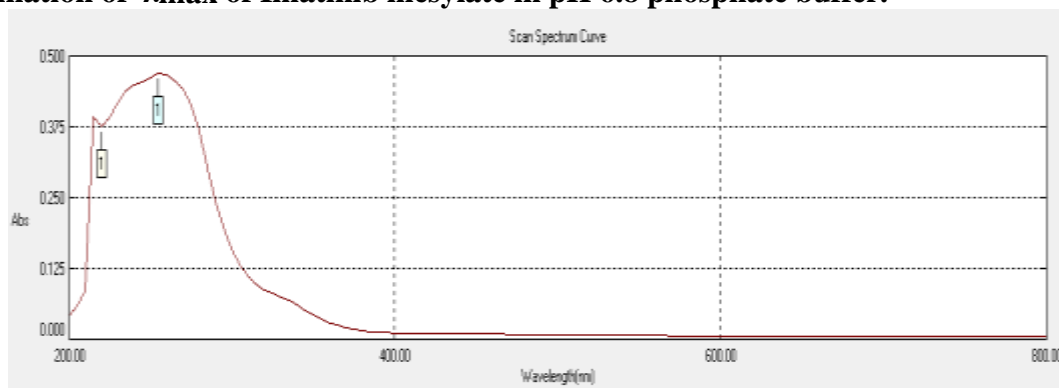
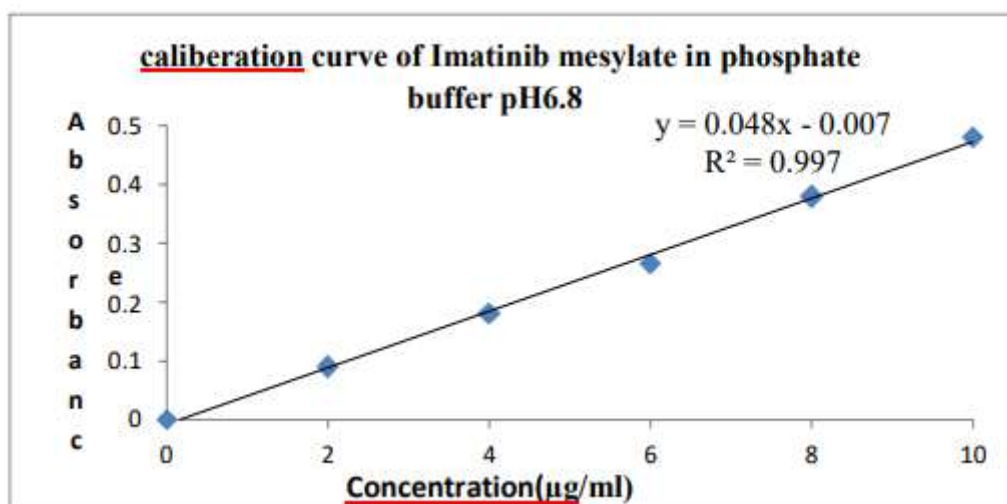


Fig 5.  $\lambda_{max}$  of Imatinib mesylate

Table 6: Maximum wavelength of Imatinib mesylate

S.no	Peak	Wavelength(nm)	Absorbance
1.	Peak	255	0.470



**Fig 6. Calibration curve of Imatinib mesylate**

**Table 7: Calibration values of Imatinib mesylate**

S.no	Concentration(µg/ml)	Absorbance(nm)*
1.	0	0
2.	2	0.09± 0.03
3.	4	0.18± 0.06
4.	6	0.265±0.04
5.	8	0.380±0.05
6.	10	0.481±0.06
7.	Slope	0.048
8.	Regression	0.997

**\*All the values are calculated as Mean ±SD, n=3**

Calibration curve of Imatinib mesylate was performed by preparing different concentrations solutions in pH6.8 phosphate buffer. The prepared concentrations absorbance was observed at 255nm using U.V-Visible spectrophotometer.

A graph was plotted by taking concentration on x-axis and absorbance on y-axis. The results represented that the prepared Imatinib mesylate dilutions using pH 6.8 follows Beers Lambert's law showing increased absorbance values with increasing concentration. The regression value is 0.997 indicating that the line passed through the origin was linear and suitable for the spectrophotometric analysis. The results were represented in table 8.

**Table 8. Evaluation parameters of Imatinib mesylate nanoparticles**

Formulation code	Percentage yield (%)*	Drug content*(%)	Entrapment efficiency (%)*	Particle size(nm)	Zeta potential (mV)	PDI
INP1	94.2	98.2±0.25	97.2 ±0.26	220.2	-26.2	1.0
INP2	68.4	64.5±0.48	57.2 ±0.45	1.13	-11.5	1.0
INP3	93.3	97.5±0.52	98.3 ±0.65	3.69	-15.7	1.0
INP4	70.2	65.4±0.89	63.6 ±0.35	295.3	-14.8	1.0
INP5	76.5	74.2±0.15	72.4 ±0.55	260.9	-3.43	1.0



INP6	75.2	72.3±0.69	70.2 ±0.41	357.9	-19.4	1.0
INP7	72.9	69.5±0.46	68.3 ±0.63	357.9	-14.6	1.0
INP8	78.7	75.4±0.85	72.3 ±0.15	2.378	-19.4	0.39
INP9	71.9	72.6±0.74	67.2 ±0.91	91.28	-14.6	1.0
INP10	80.2	81.4±0.19	76.4 ±0.68	255	-17.5	1.0
INP11	82.3	79.8±0.26	77.3 ±0.88	357.9	-14.8	1.0
INP12	85.3	82.4±0.49	80.5 ±0.98	357.9	-14.8	1.0
INP13	77.8	76.8±0.67	75.7 ±0.75	172.2	-14.3	1.0
INP14	79.6	77.3±0.75	76.6 ±0.65	2.52	-6.78	1.0
INP15	89.5	89.2±0.95	88.3 ±0.45	106.6	-7.08	1.0
INP16	78.9	75.2±0.48	70.1 ±0.33	342	-12.3	1.0
INP17	72.4	68.4±0.25	64.8 ±0.64	357.9	-14.8	1.0

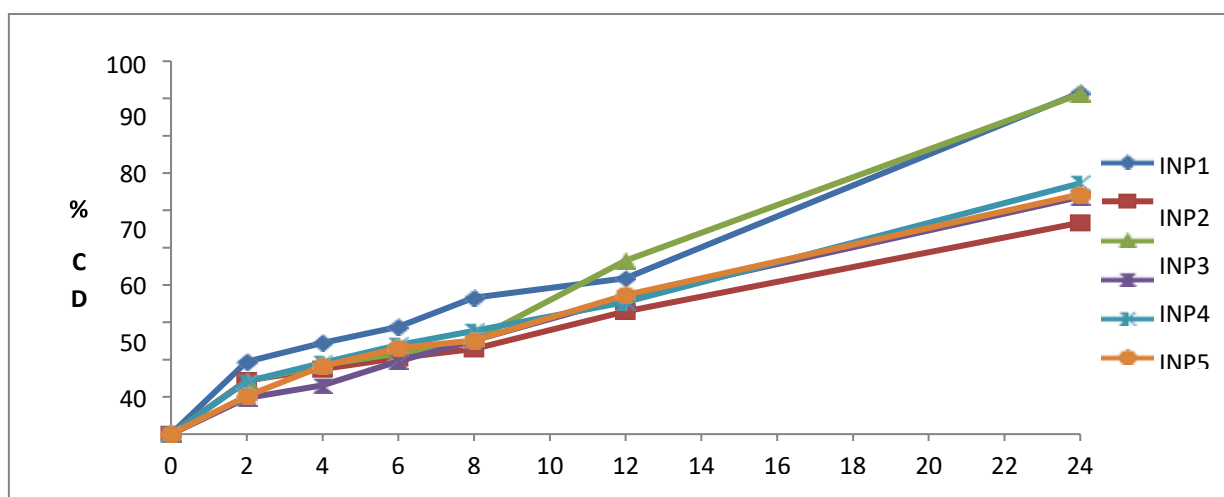
**\*All the values are calculated as Mean± SD, n=3**

The formulated nanoparticles are evaluated for parameters like percentage yield, entrapment efficiency, particle size, zeta potential and PDI. Here all the formulations are prepared with different drug: polymer ratio, rpm, and stabilizer. These changes show different yields, Entrapment efficiency, particle size, Polydispersity index. As the rpm increases the particle size decreased, entrapment efficiency also varied. Percentage yield results were in the range of 64.8.2- 98.2%, entrapment efficiency was in the range of 64.5-98.3% and particle size in the range of 220.2-502.4nm, Drug content range 64.5-98.2 %, zeta potential range -3.43-26.2mV, PDI range 0.39-1.0. The particle size and zeta potential indicated that the particles.

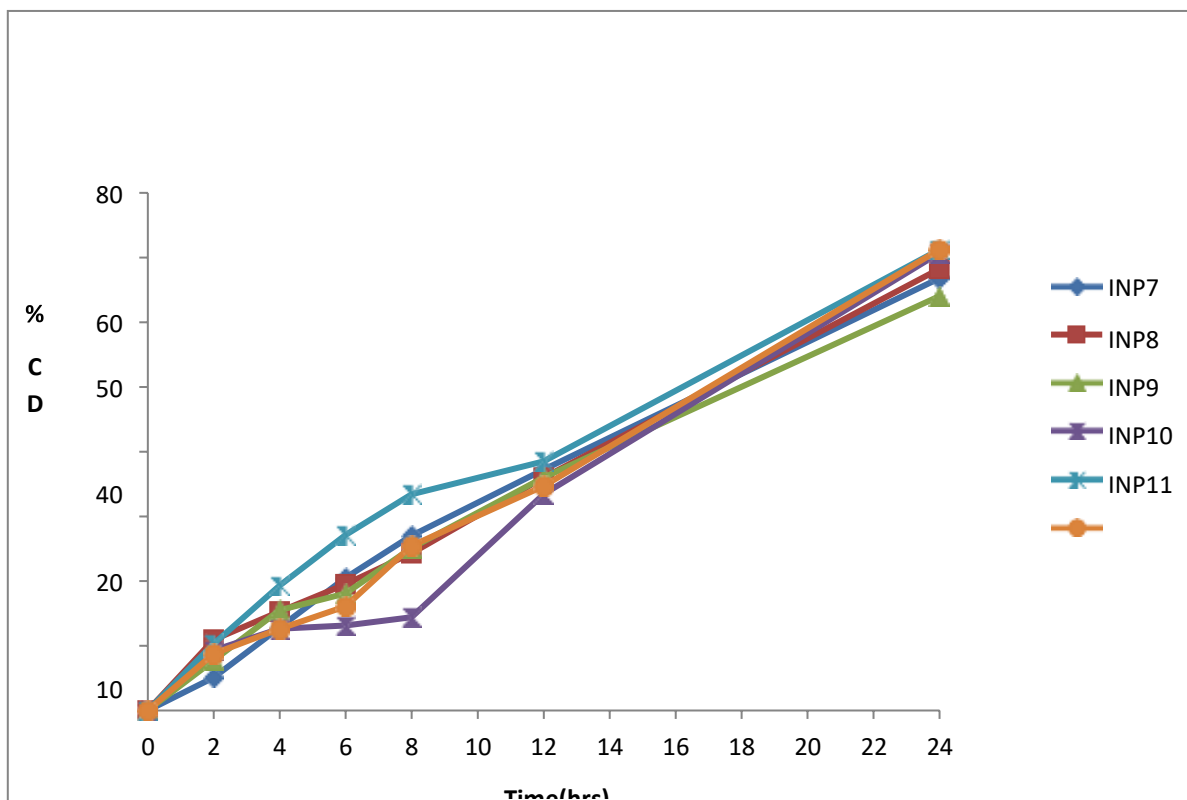
This repelling property was thought to be useful in decreasing Opsonization and favors target specificity.

**Table 9: *In-vitro* drug release studies**

Formulation code	%CDR					
	Time (hrs)					
	2	4	6	8	12	24
INP1	19.4±0.25	24.5±0.65	28.8±0.12	36.6±0.98	41.7±0.56	91.5±0.68
INP2	14.4±0.36	17.4±0.98	20.4±0.16	26.9±0.59	32.9±0.58	56.7±0.48
INP 3	14.1±0.78	18.6±0.35	21.6±0.75	25.2±0.32	46.5±0.85	91.2±0.1
INP4	9.7±0.18	13.1±0.36	19.5±0.75	25.1±0.25	36.6±0.69	63.6±0.45
INP5	14.6±0.81	19.6±0.95	23.9±0.15	27.7±0.85	35.4±0.12	67.2±0.65
INP6	10.2±0.52	18.2±0.48	23.1±0.62	25.1±0.25	37.2±0.25	64.2±0.35
INP7	5.1±0.58	12.8±0.35	20.5±0.26	27.3±0.45	38.2±0.41	66.8±0.16
INP8	7.7±0.22	15.2±0.33	18.7±0.47	25.8±0.63	36.1±0.98	69.8±0.86
INP9	9.2±0.59	16.8±0.62	20.5±0.59	29.4±0.23	39.8±0.81	70.7±0.78
INP10	10.1±0.32	12.6±0.38	13.1±0.41	14.4±0.45	33.4±0.28	72.3±0.51
INP11	10.2±0.55	19.2±0.65	27.1±0.61	33.4±0.59	38.5±0.41	74.2±0.32
INP12	8.7±0.25	12.6±0.36	16.1±0.65	25.4±0.72	34.7±0.23	75.7±0.78
INP13	7.7±0.82	14.5±0.89	21.8±0.56	27.7±0.36	37.1±0.56	71.2±0.28
INP14	9.1±0.26	16.7±0.39	23.1±0.45	28.2±0.55	36.1±0.78	69.2±0.55
INP15	12.3±0.22	19.9±0.35	31.3±0.58	36.5±0.26	46.8±0.56	87.8±0.85
INP16	9.3±0.78	15.4±0.82	21.8±0.69	28.2±0.45	37.2±0.69	68.8±0.25
INP17	7.8±0.36	12.2±0.39	17.3±0.59	22.1±0.98	28.6±0.56	60.2±0.48

(All the values are calculated as Mean  $\pm$  S.D, n=3)Fig 7. *In-vitro* drug release studies of Imatinib mesylate nanoparticles (INP1-INP6)

By using the Design expert software 17 formulations are prepared and the *in-vitro* drug release studies were performed and discussed in the experimental procedure. The 17 formulations are prepared by varying Drug: polymer ratio, concentration of stabilizer and rpm. *In-vitro* drug release studies were performed up to 24 hrs. The INP1 with 1:1 ratio, 0.95 stabilizer, and rpm 3000 had shown the drug release of 91.5% up to 24 hrs. The INP2 with 1:1 ratio, 0.95 stabilizer, and rpm 1000 had shown the drug release of 56.7% up to 24 hrs. The INP3 with 1:1 ratio, 0.4 stabilizer, and rpm 2000 had shown the drug release of 91.2% up to 24 hrs. The INP4 with 1:5.5 ratio, 0.4 stabilizer, and rpm 3000 had shown the drug release of 63.6% upto 24 hrs. The INP5 with 1:5.5 ratio, 1.5 stabilizer, and rpm 3000 had shown the drug release of 67.2 up to 24 hrs. The INP6 with 1:5.5 ratio, 0.95 stabilizer, and rpm 2000 had shown the drug release of 64.2 up to 24 hrs.

Fig. 8. *In-vitro* drug release studies of Imatinib mesylate nanoparticles (INP7-INP12)

The INP7 with 1:5.5 ratio, 0.95% stabilizer, at 2000 rpm had shown the drug release of 66.8% up to 24 hrs. The INP8 with 1:1 ratio, 0.95% stabilizer, at 1000 rpm had shown the drug release of 69.8% up to 24 hrs. The INP9 with 1:10 ratio, 0.4% stabilizer, at 2000 rpm had shown the drug release of 70.7% up to 24 hrs. The INP10 with 1:1 ratio, 1.5% stabilizer, at 2000 rpm had shown the drug release of 72.3% up to 24 hrs. The INP11 with 1:5.5 ratio, 0.95% stabilizer, at 2000 rpm had shown the drug release of 74.2 up to 24 hrs. The INP12 with 1:5.5 ratio, 0.95% stabilizer, at 2000 rpm had shown the drug release of 75.7 up to 24 hrs.

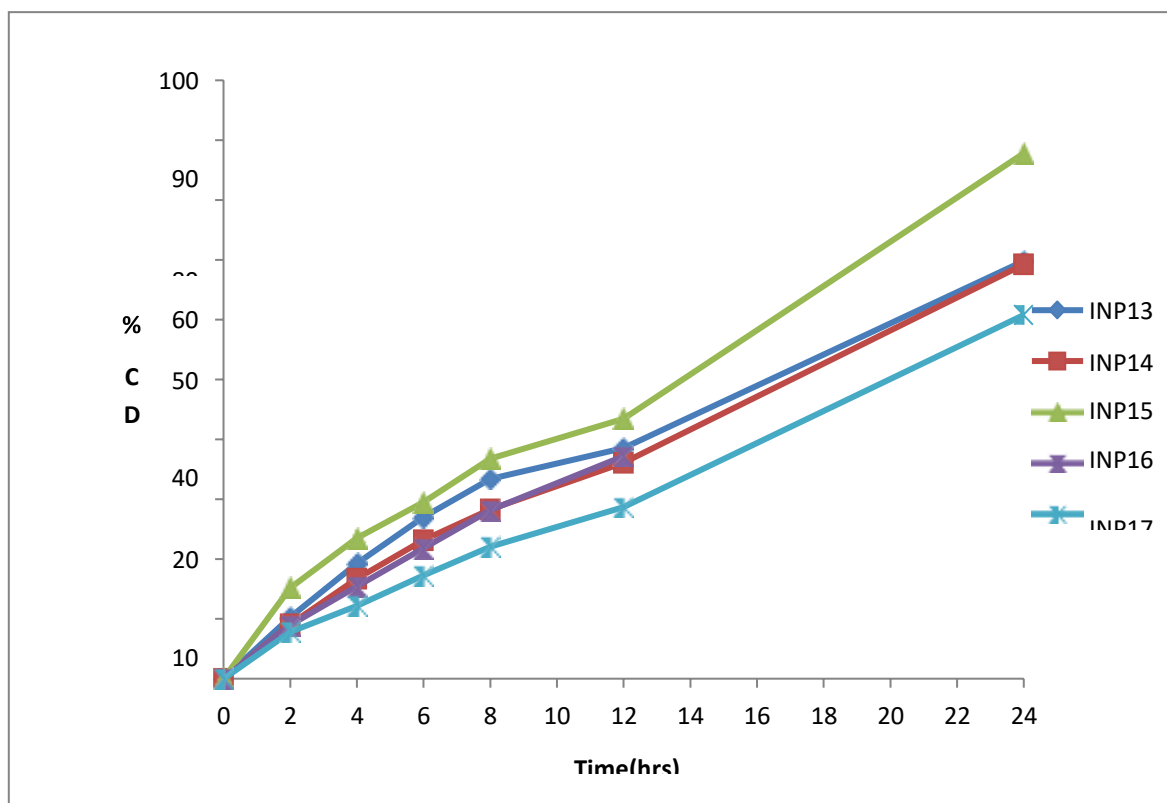


Fig. 9 *In-vitro* drug release studies of Imatinib mesylate nanoparticles (INP13-INP17)

The INP13 with 1:10 ratio, 0.95% stabiliser, at 1000rpm had shown the drug release of 71.2% up to 24 hrs. The INP14 with 1:10 ratio, 0.4% stabiliser, at 1000 rpm had shown the drug release of 69.2% up to 24 hrs. The INP15 with 1:5.5 ratio, 1.5% stabiliser, at 2000 rpm had shown the drug release of 87.8% up to 24 hrs. The INP16 with 1:5.5 ratio, 0.4% stabiliser, at 1000 rpm had shown the drug release of 68.8% up to 24 hrs. The INP17 with 1:5.5 ratio, 0.95% stabiliser, at 2000 rpm had shown the drug release of 60.8 up to 24 hrs.

## Show the contour plots of Response 1(AB)

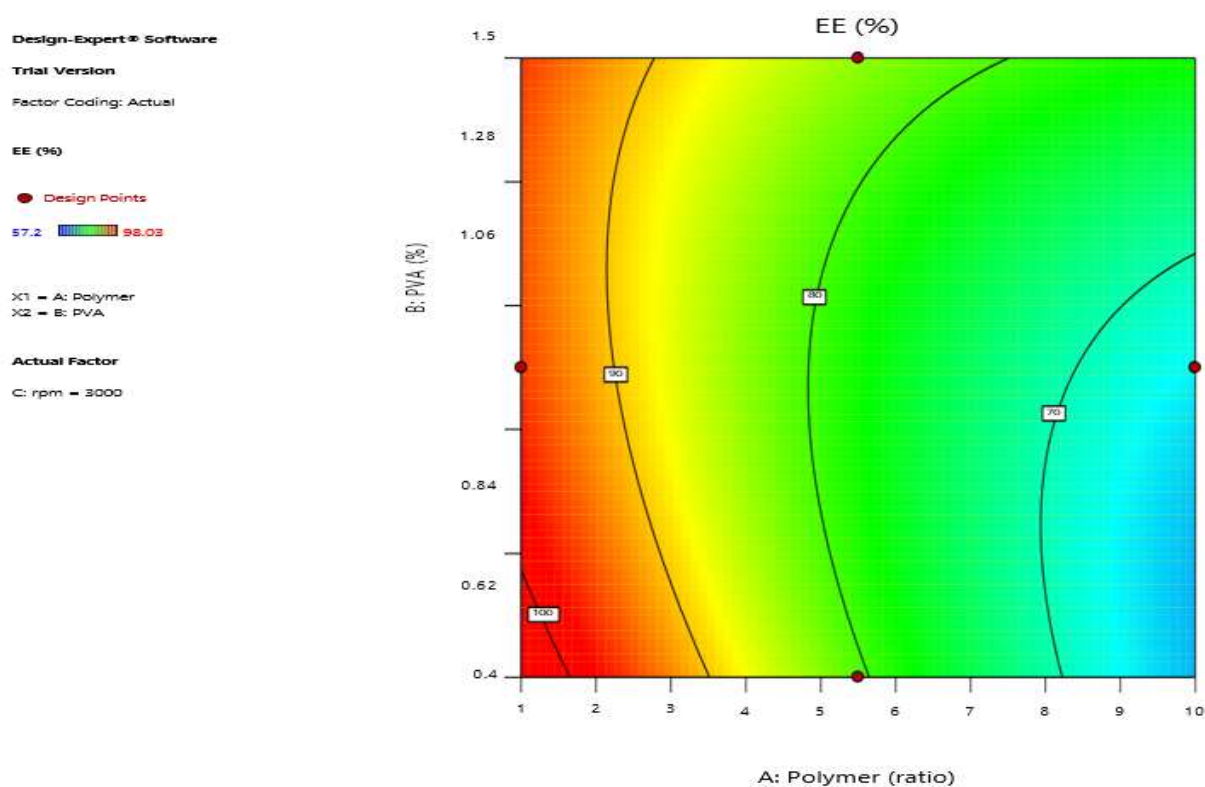


Fig 10. Shows the Contour plots of response 1(AB)

## Shows the Contour plot of response1 (AC)

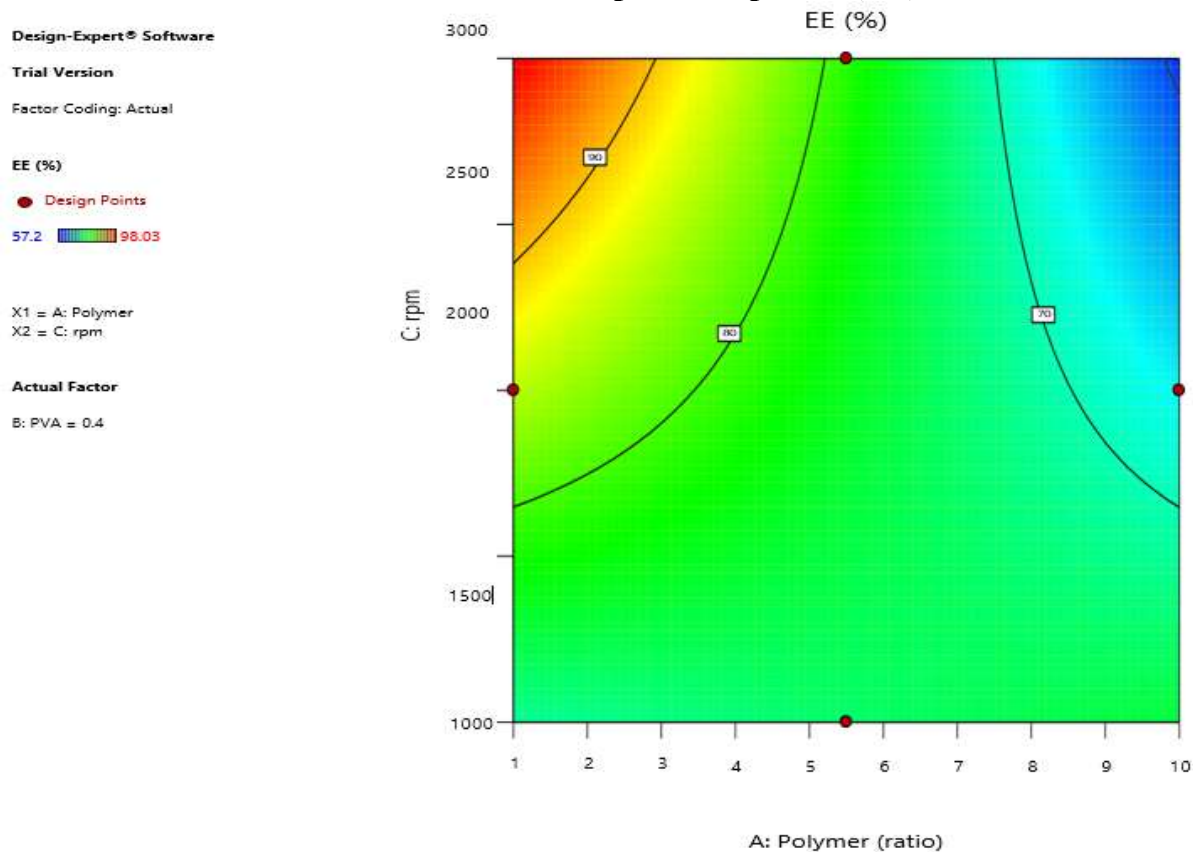


Fig. 11 Shows the Contour plots of response 1(AC)

Shows the contour plots of response 1(BC)

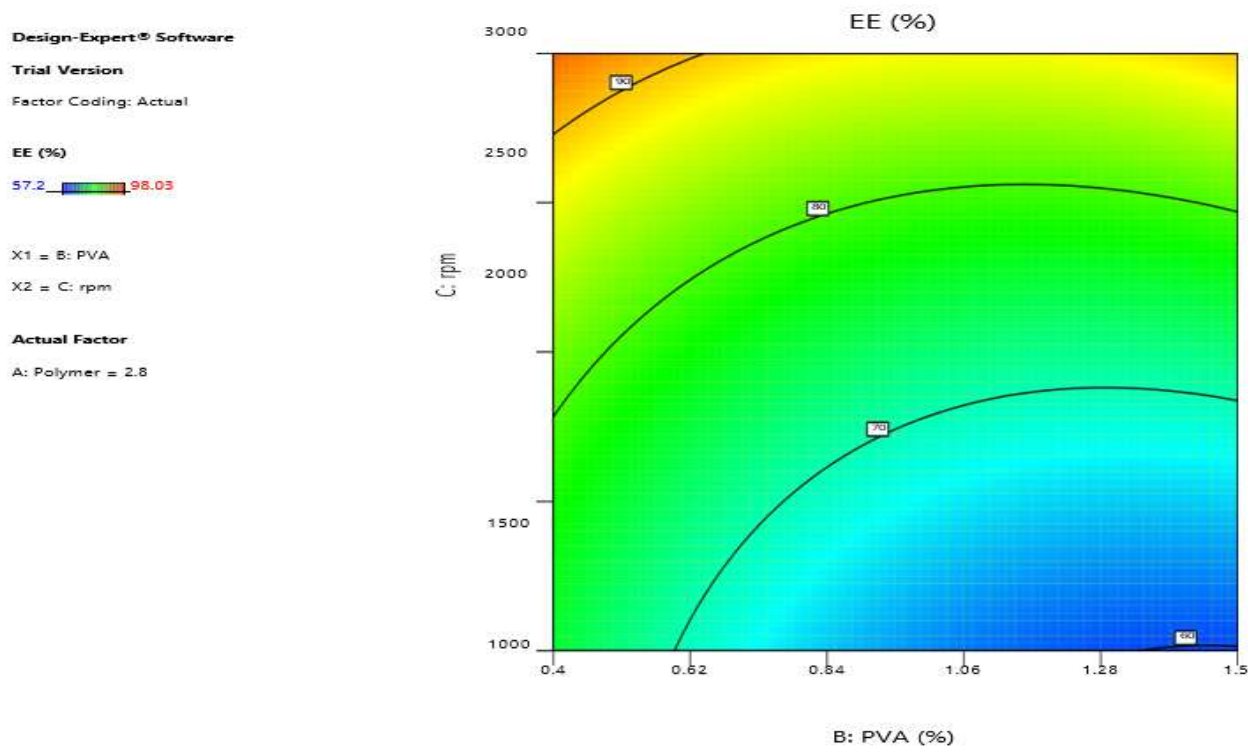


Fig. 12. Shows the contour plots of response 1(BC)

Shows the 3D graph of response1(AB)

Fig. 13. Shows the 3D surface of response 1(AB)

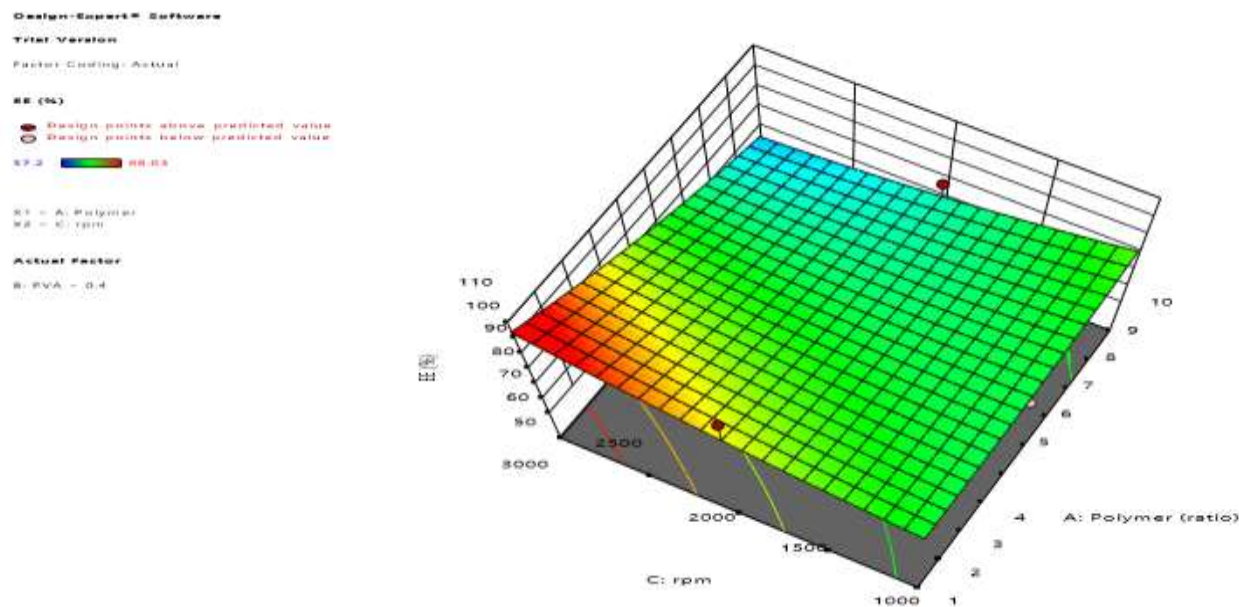


Fig.14. Shows the 3D surface of response 1(AC)

Shows the 3D graph of response 1(BC)

Fig 15. Shows the 3D surface of response1 (BC)

The above graphs represent the response 1(Entrapment efficiency). In the graphs of AB (contour&3Dsurface) represents as the stirring speed increases, the entrapment efficiency also increases. In the graphs of AC, represents as the concentration of stabiliser is minimum, the



entrapment efficiency increases. In the graphs of BC, as the drug: polymer ratio is minimum, higher percentage of entrapment efficiency is obtained.

**Shows the contour plots of response 2(AB)**

**Shows the contour plots of response 2(AB)**

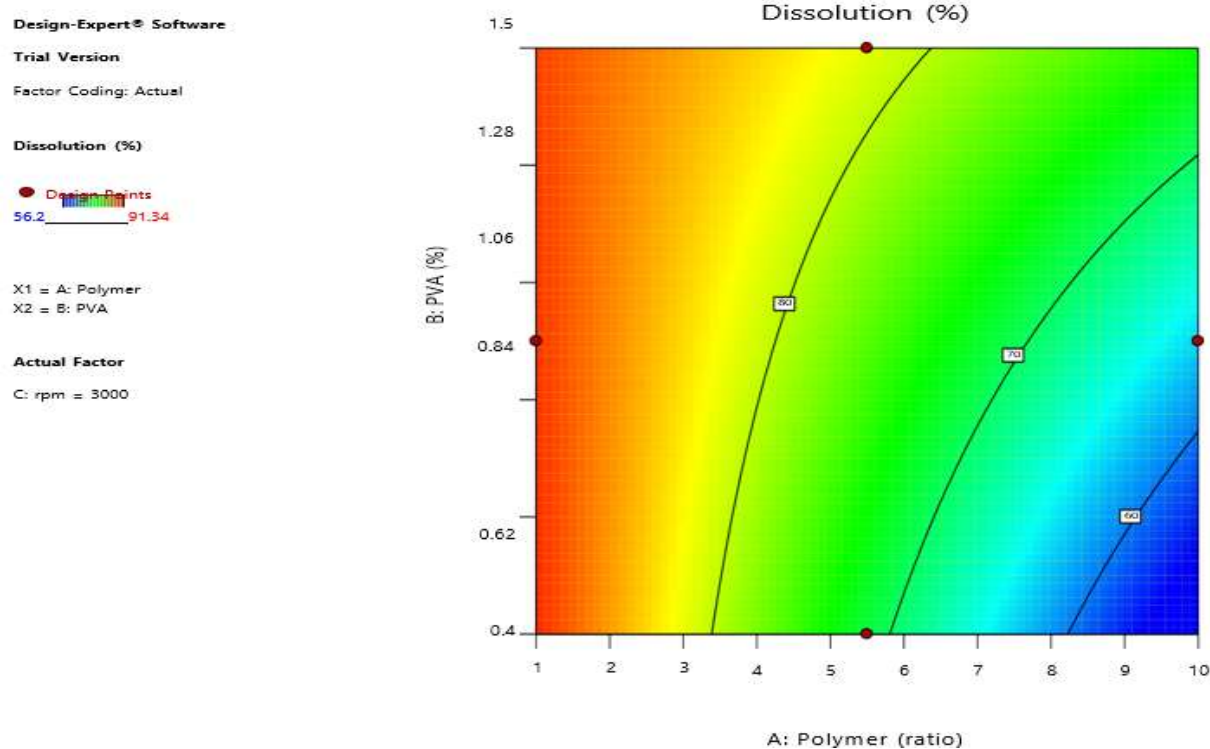


**Fig 16. Shows the contour plots of response2 (AB)**

**Shows the contour plots of response 2(AC)**

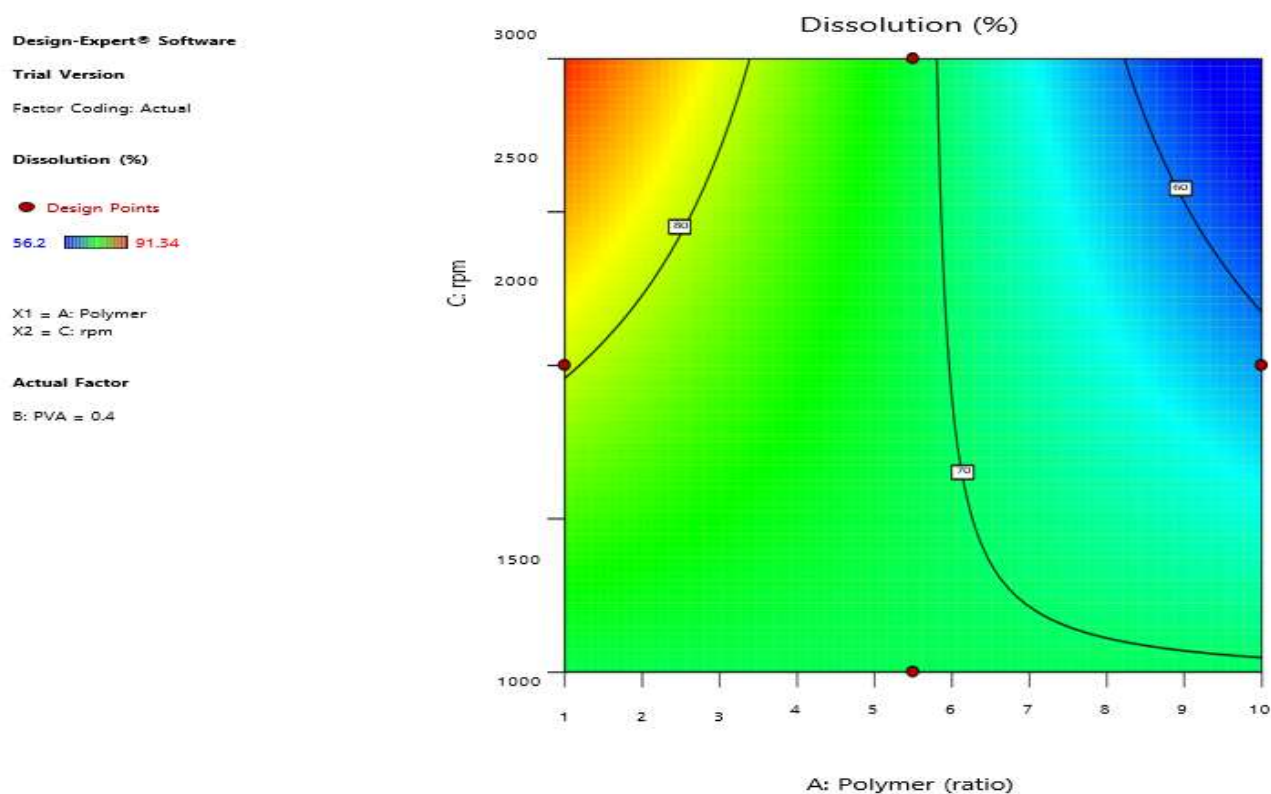


**Fig. 17. Shows the contour plots of response2 (AC)**

## Shows the contour plots of response 2(BC)

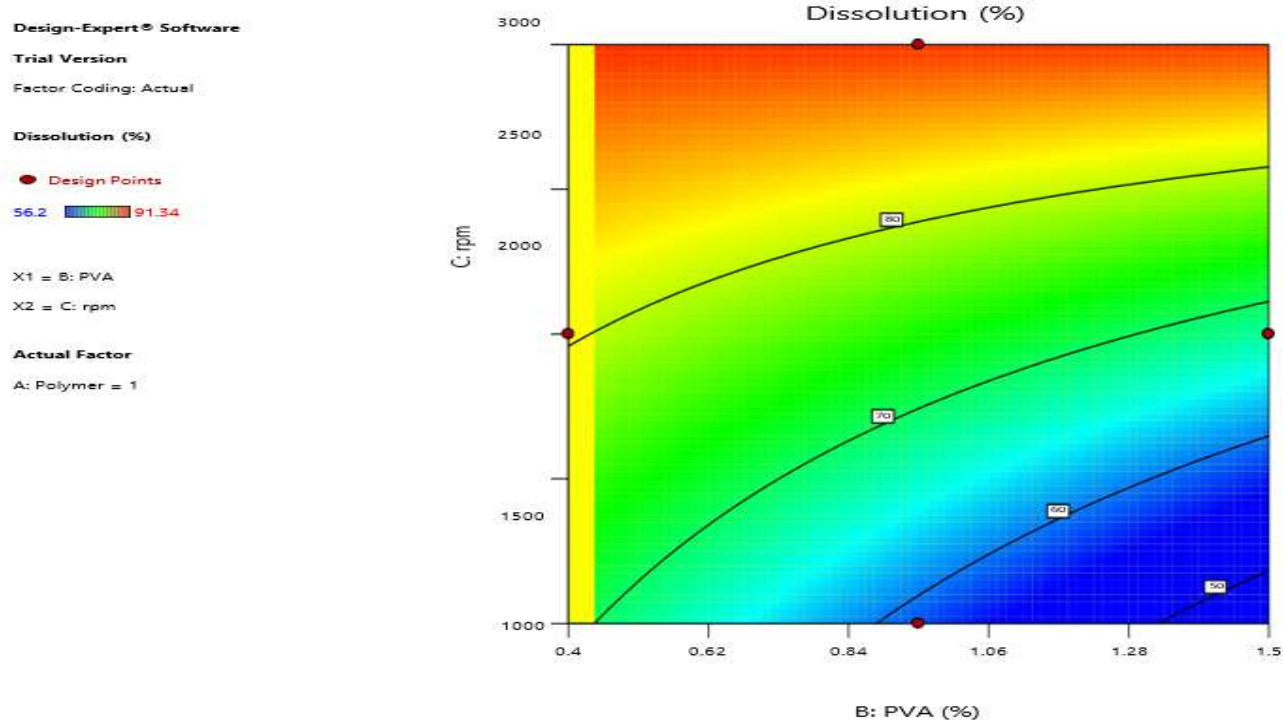


Fig 18. Shows the contour plots of response2(BC)

## Shows the 3D graph of response2(AB)

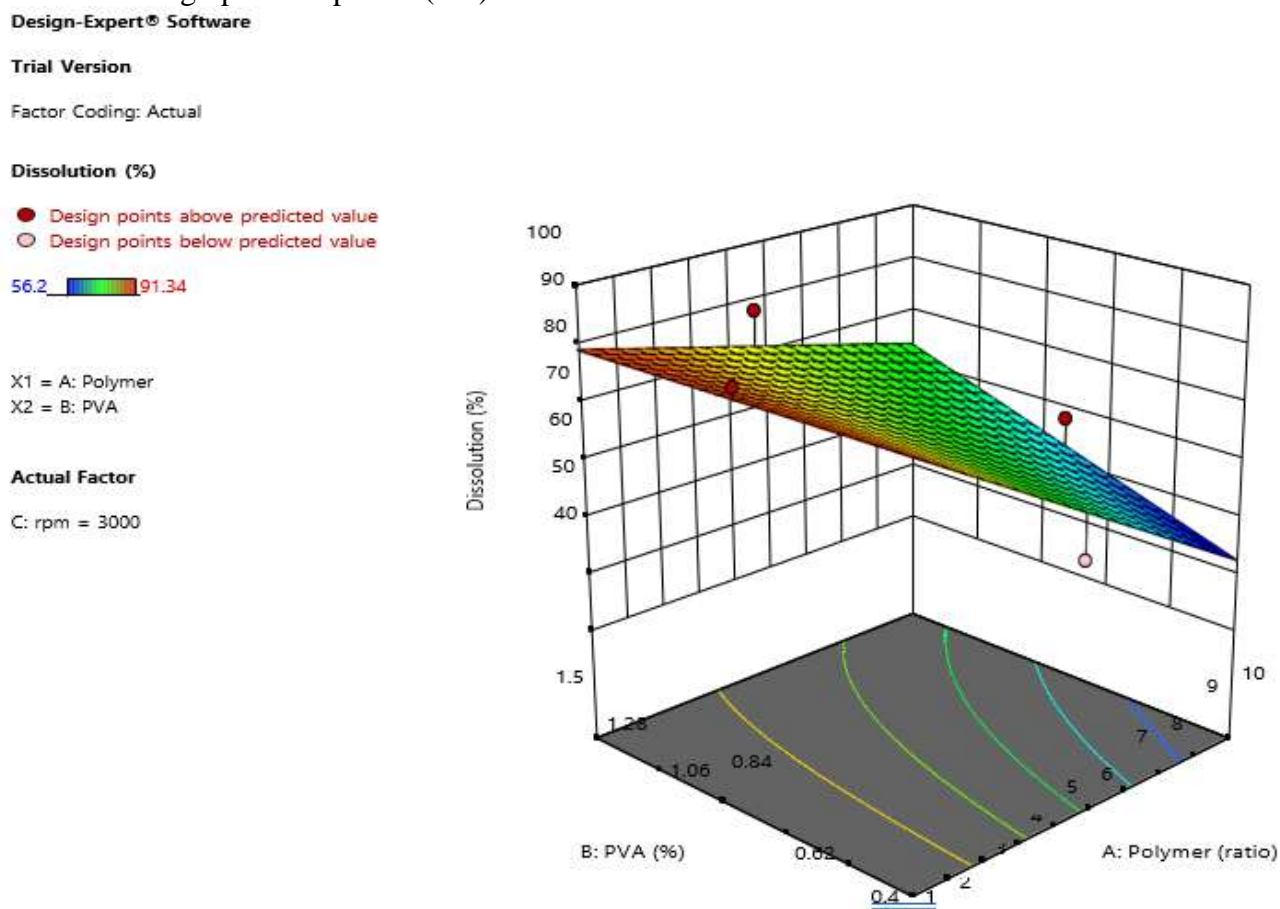


Fig. 19. Shows the 3D surface of response2(AB)

## Shows the 3D surface of response 2(AC)

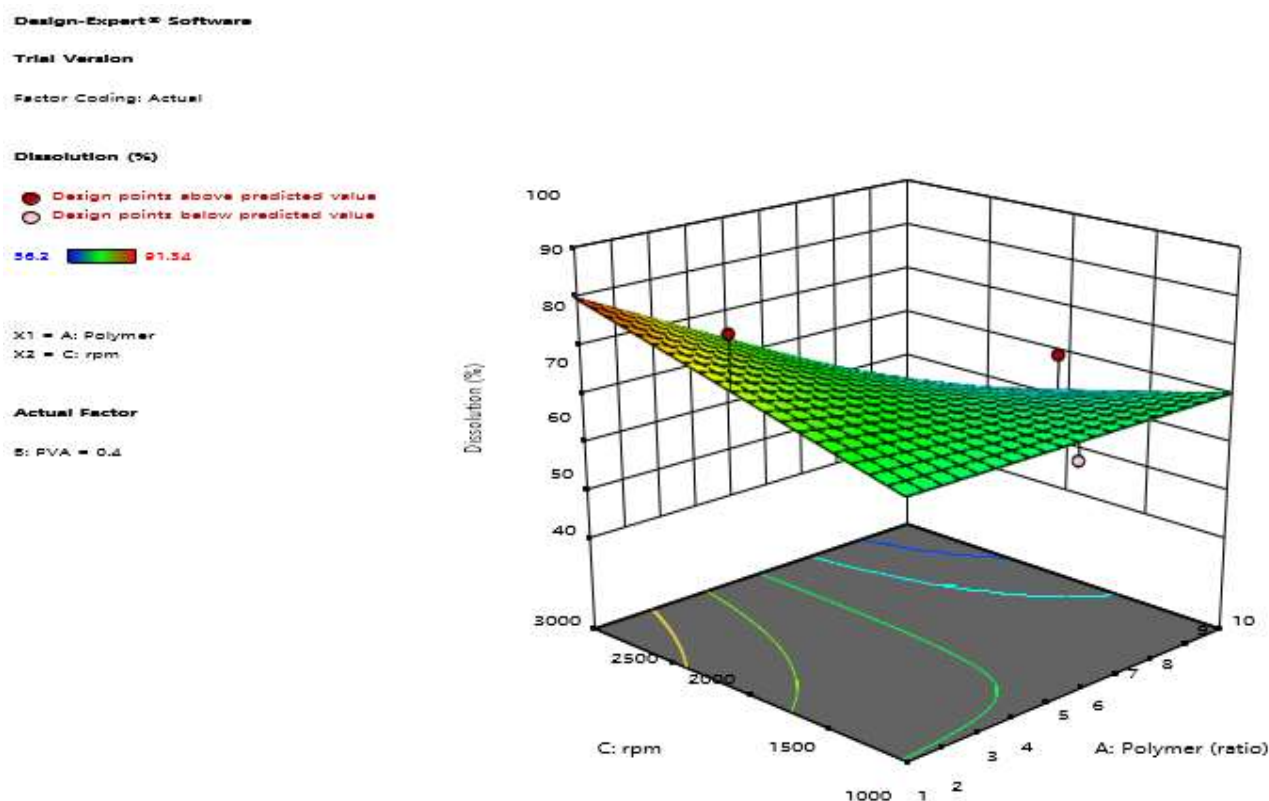


Fig. 20. Shows the 3D surface of response2 (AC)

## Shows the 3D surface of response 2(BC)

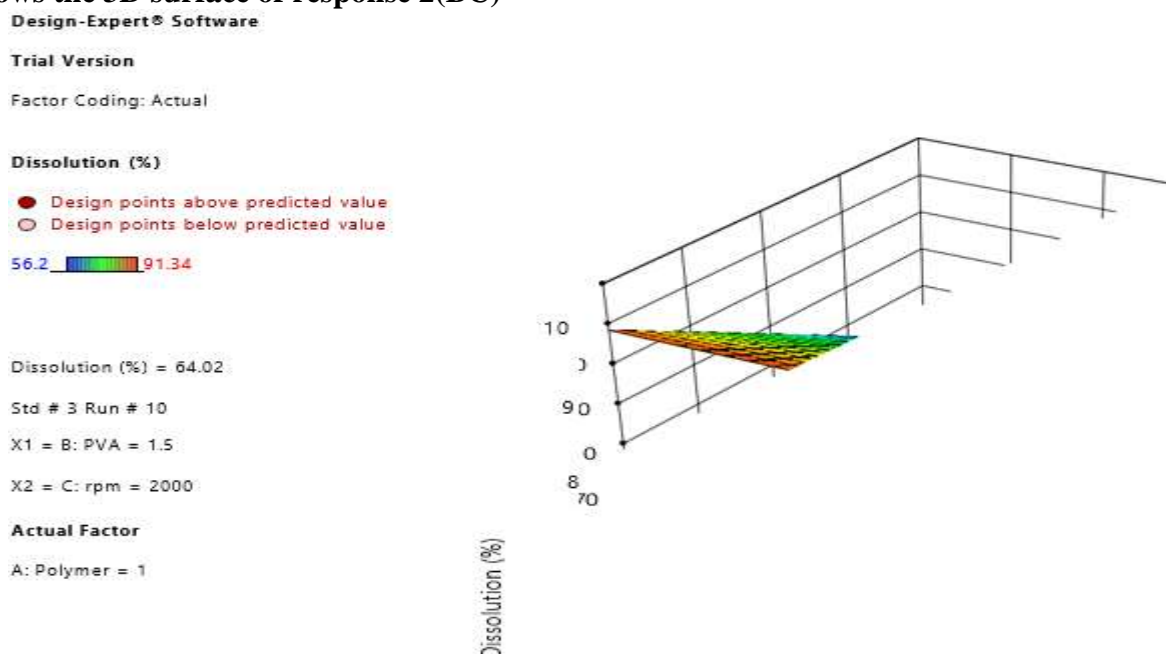


Fig. 21. Shows the 3D surface of response2 (BC)

The above graphs represent the response 2(in-vitro drug release studies). In the graphs of AB (contour&3D surface) represents as the stirring speed increases, the drug release also increases. In the graphs of AC, represents as the concentration of stabiliser is minimum, the drug release increases. In the graphs of BC, as the drug: polymer ratio is minimum, higher percentage of drug release is obtained.



**Table 11. Anova table for entrapment efficiency**

Std. Dev	10.47	R <sup>2</sup>	0.6013
		Adeq. Precision	4.1109

A negative Predicted R<sup>2</sup> implies that the overall mean may be a better predictor of your response than the current model. In some cases, a higher order model may also predict better.

Adeq Precision measures the signal to noise ratio. A ratio greater than 4 is desirable. Your ratio of 4.1109 indicates an adequate signal. This model can be used to navigate the design space.

**Table 12. Anova Table for In-Vitro Drug Release Studies**

Std. Dev	8.01	R <sup>2</sup>	0.6211
		Adeq. Precision	6.3575

Adeq Precision measures the signal to noise ratio. A ratio greater than 4 is desirable. Your ratio of 6.3575 indicates an adequate signal. This model can be used to navigate the design space.

**Table 13: Intercept and p value of each factor for response of entrapment efficiency and in-vitro drug release studies**

	Intercept	A	B	C	AB	AC	BC	A <sup>2</sup>	B <sup>2</sup>	C <sup>2</sup>
<b>EE</b>	69.648	-3.462	-1.54	5.647	5.3575	-10.8525	2.882	3.469	4.164	2.514
<b>p-values</b>		0.380	0.688	0.170	0.340	0.0768	0.598	0.5182	0.441	0.63
<b>Dissolution</b>	70.0518	-3.933	-0.918	<b>6.317</b>	5.492	<b>-9.175</b>	6.02			
<b>p-values</b>		0.1950	0.75	<b>0.049</b>	0.200	<b>0.0450</b>	0.1638			

#### Quadratic equation for Entrapment efficiency

$R_1 = 69.45 - 3.46 * A - 1.55 * B + 5.65 * C + 5.36 * AB - 10.85 * AC + 2.88 * BC + 3.47 * A^2 + 4.16 * B^2 + 2.51 * C^2$  (\* indicates, A= Drug: Polymer ratio, B=Concentration of Stabiliser, C=stirring speed,

From the above quadratic equation, factor A that is Drug: polymer ratio as negative sign. This indicates as drug: polymer ratio decreases, entrapment efficiency increases. For factor B that is concentration of stabiliser as negative sign. This indicates as concentration of stabiliser decreases, entrapment efficiency increases. For factor C that is stirring speed as positive sign. This indicates as stirring speed increases, entrapment efficiency increases. For factor AB as positive sign. This indicates as the concentrations of AB increases, entrapment efficiency decreases. But to obtain high entrapment efficiency the concentration of AB factor is to be decreased. For factor AC as negative sign, to obtain high entrapment efficiency the factor A is to be decreased and the factor C is to be increased. For Factor BC as positive sign, to obtain high entrapment efficiency the concentration of stabiliser is to be decreased and the stirring speed is to be increased.

#### Quadratic equation for In-vitro drug release studies

$R_2 = 70.05 - 3.93 * A - 0.9188 * B + 6.32 * C + 5.49 * AB - 9.18 * AC + 6.02 * BC$ .

From the above quadratic equation, factor A that is Drug: polymer ratio as negative sign. This indicates as drug: polymer ratio decreases, % of drug release increases. For factor B that is concentration of stabiliser as negative sign. This indicates as concentration of stabiliser decreases, % of drug release increases. For factor C that is stirring speed as positive sign. This indicates as stirring speed increases, % of drug release increases. For factor AB as positive sign. This indicates as the concentrations of AB increases, % of drug release decreases. But to obtain higher % of drug release, the concentration of

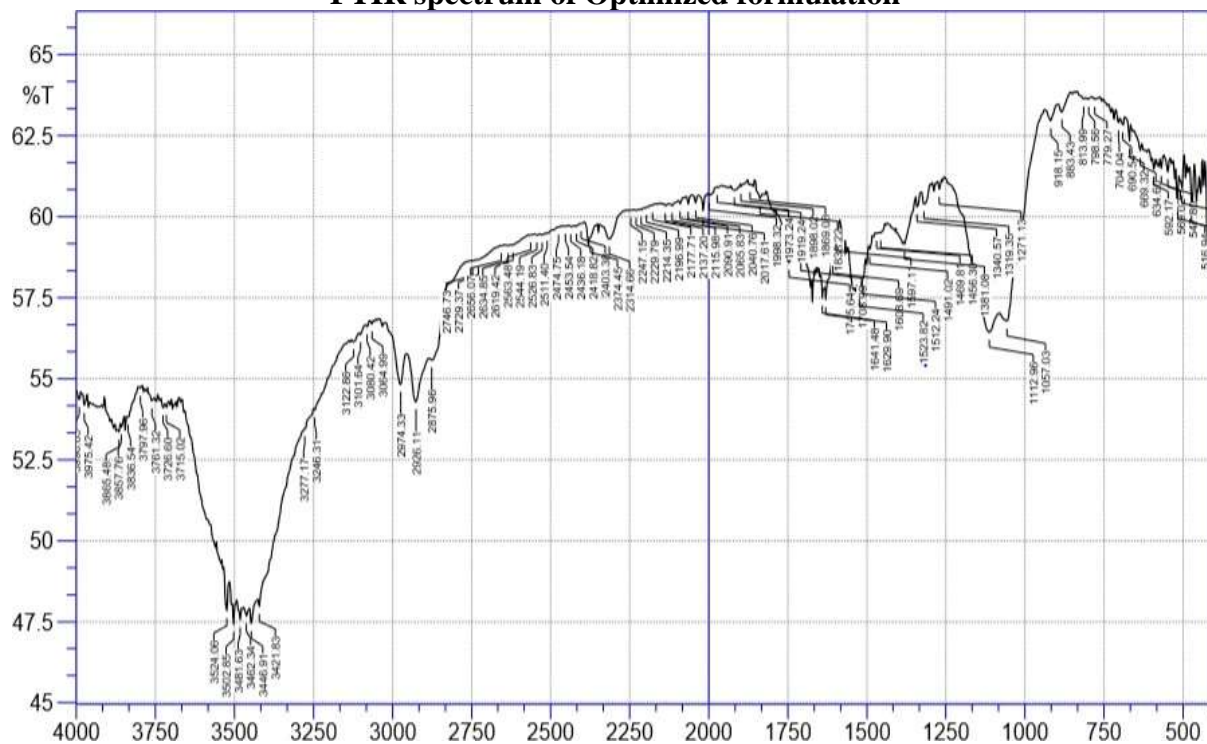
AB factor is to be decreased. For factor AC as negative sign, to obtain higher % of drug release the factor A is to be decreased and the factor C is to be increased. For Factor BC as positive sign, as the factor BC increases, the % of drug release decreases. But to obtain higher % of drug release the concentration of stabiliser is to be decreased and the stirring speed is to increase. After fitting the data of 17 formulations in the Box- Behnken Design, the Optimized formulation was obtained.

**Table 14: Optimized Formulation**

Factor	Name	Level	Low Level	High Level
A	Polymer	1.00	1:1	1:10.00
B	PVA	0.4	0.4	1.5
C	Stirring speed	3000	1000	3000`

**Table 15: Point Prediction**

Response	Predicted Mean
Entrapment efficiency (%)	99.78
Drug release (%)	99.86

**FTIR spectrum of Optimized formulation****Fig. 22. FTIR Spectrum of Optimized formulation.****Table 16: Characteristic peaks observed for Optimized formulation.:**

S.NO	Type of Bond	Actual frequency(cm <sup>-1</sup> )	Observed frequency(cm <sup>-1</sup> )	Conformation
1.	CH stretching	2800-2900	2875.96	methyl
2.	NH stretching	3300-3500	3481.91	Amide
3.	C=O stretching	1745-1775	1745.64	Ketone
4.	C=C stretching	1475-1600	1597.211	Aromatic C=C
5.	C-H stretching(CH <sub>3</sub> )	2800-2950	2875.96	Aromatic C-H

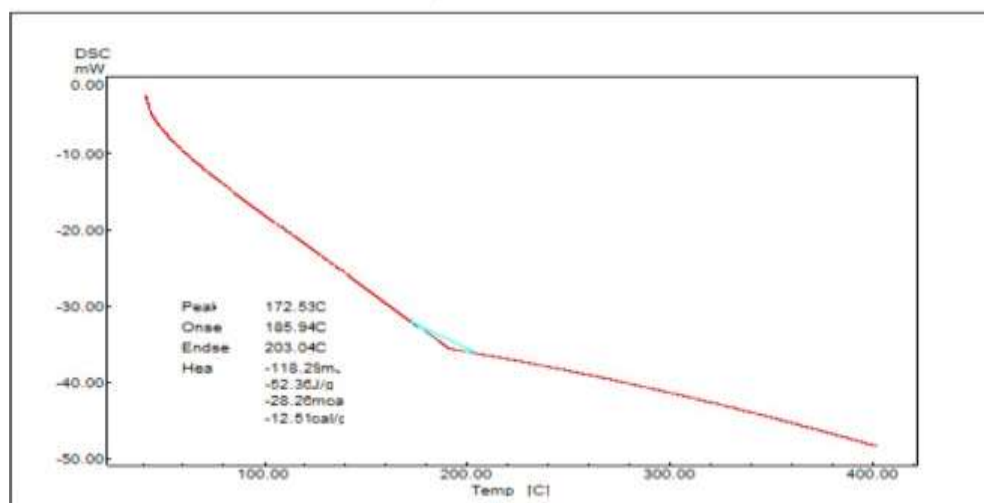


**Fig. 23 Thermogram of Optimized formulation**

The DSC study for optimized formulation was performed and shown in the figure. 23. The study starts from zero and extended up to 400°C. The peak onset is at 172.53°C and end set at 203.4 °C with peak at 185.94°C indicating that the polymer peak (Ethyl cellulose) and thus indicating successful entrapment of drug in polymer coat.

**Table 17. Evaluation Parameters of Optimized formulation**

Formulation code	Percentage yield (%)	Entrapment efficiency (%)	Particle size (nm)	Zeta potential (mV)	PDI
INP18	96.5%	99.3	502.4	-20.4	0.919

**Table 18: *In-vitro* drug release studies of Optimized formulation**

Time (hrs)	%CDR
2	14.4±0.35
4	21.2±0.48
6	28.5±0.68
8	32.1±0.35
12	48.8±0.25
24	97.42±0.62

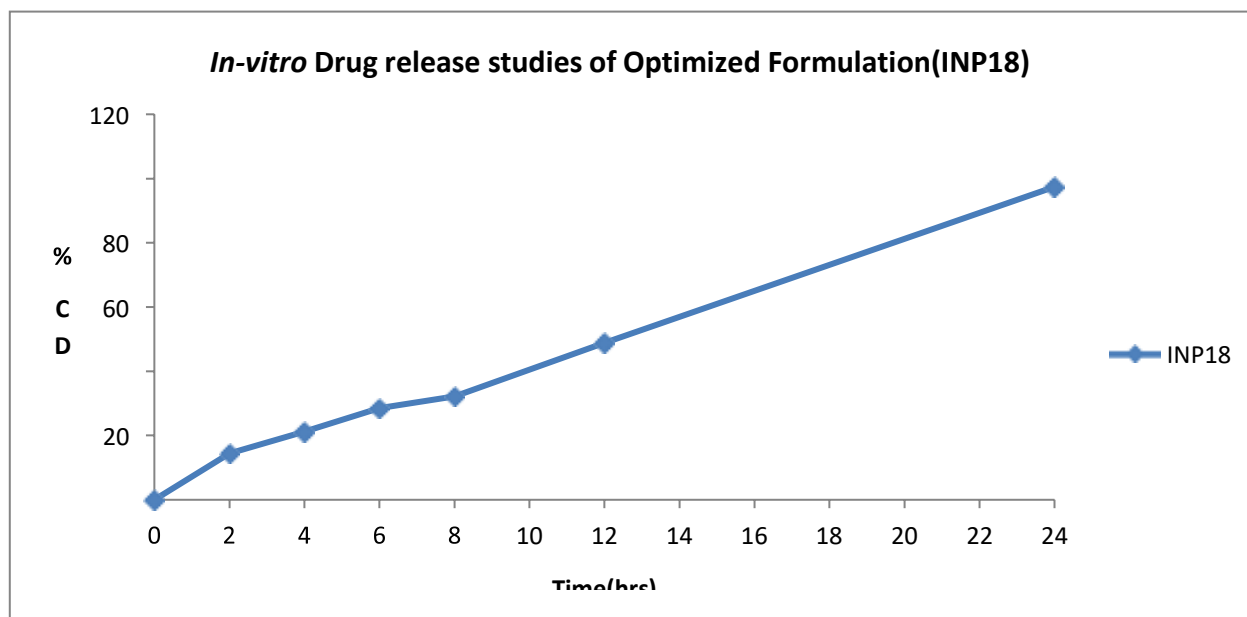


**Fig. 24 *In-vitro* drug release studies of Optimized formulation**

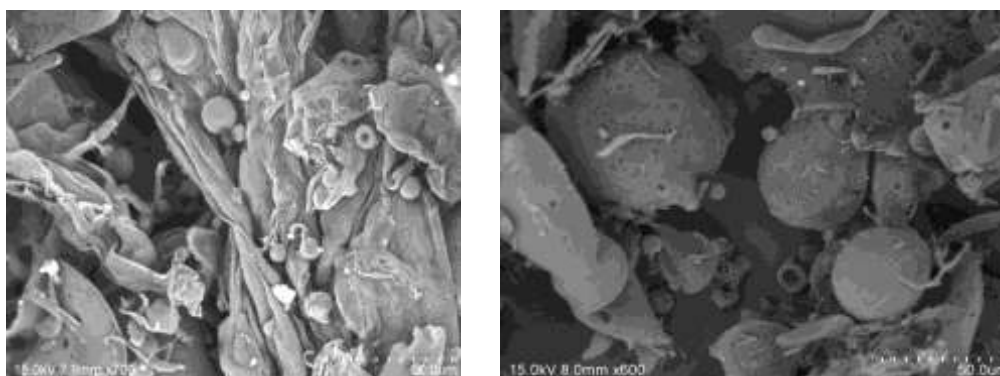
**Table 19: Response of Optimized formulation**

Response	Predicted Mean	Observed Mean	Observed std. deviation
%EE	99.78	99.3	0.339
% <i>In-Vitro</i> drug release	99.86	97.42	1.725

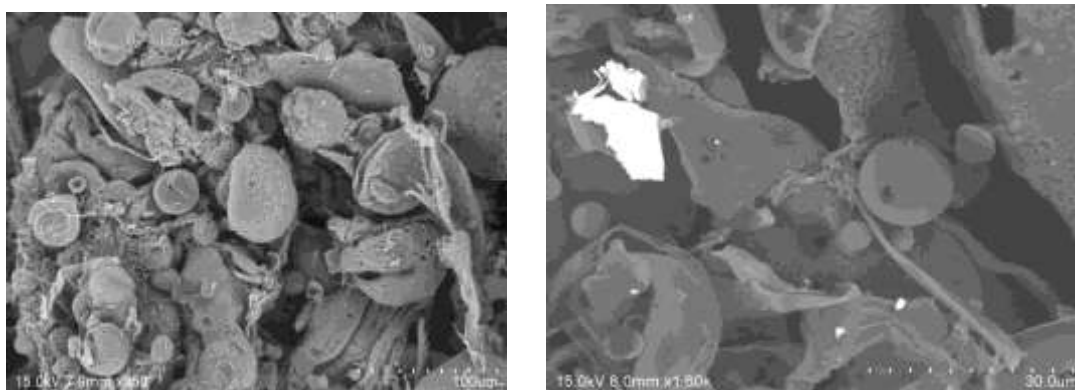
The obtained values of the optimized formulation with entrapment efficiency 99.3%, *In-vitro* 97.42% were used to calculate the std. deviation between predicted and observed mean values as represented in Table 19.

### SCANNING ELECTRON MICROSCOPY

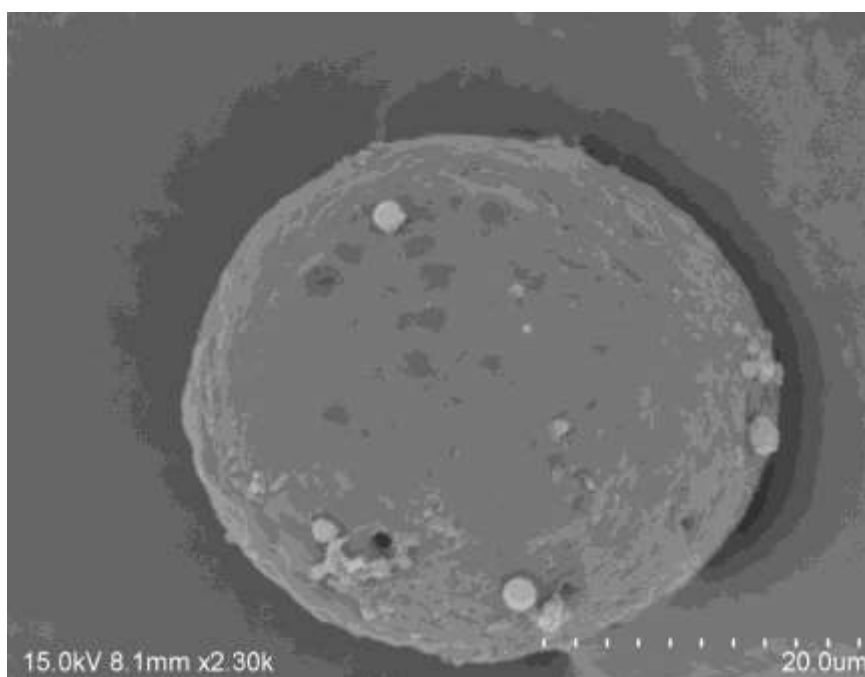
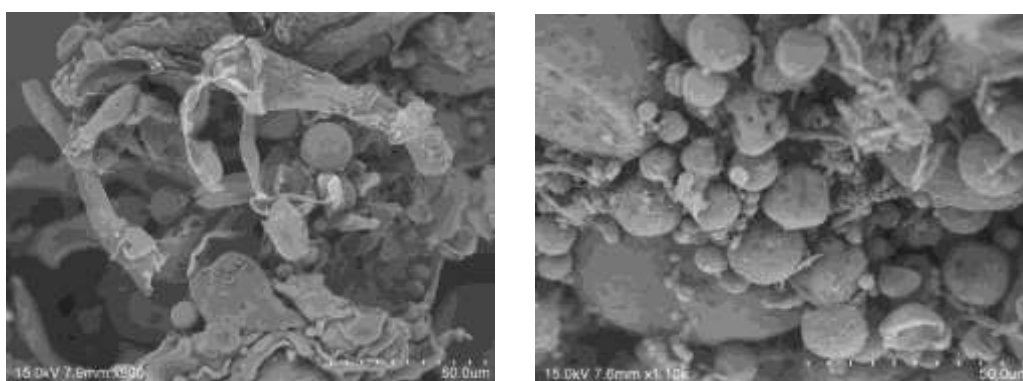
The Nanoparticles are prepared by solvent evaporation method which are investigated by SEM. The SEM photographs of the prepared formulations are shown below.



**Fig. 25. SEM photographs of INP1 formulation**

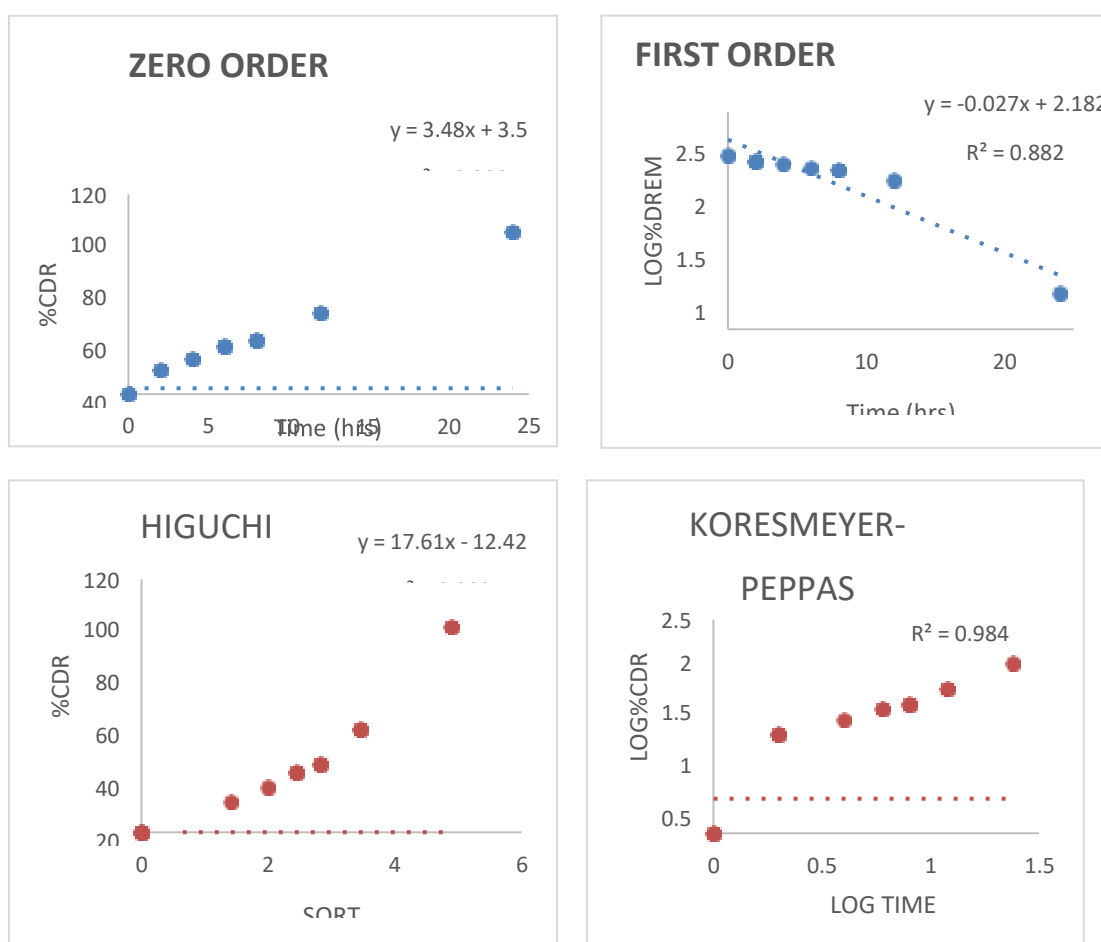


**Fig 26. SEM studies of prepared formulations (INP3)**



**Fig. 27. SEM studies of Optimized formulation**

From the results, the nanoparticles have a smooth spherical shape. Their smooth surface reveals the complete removal of solvent from the formulated nanoparticles, indicating their good quality.

***In-vitro* drug release kinetics of INP18 (Optimized formulation)**

Shows the *In-vitro* drug release kinetics of INP18 formulation.

The *In-vitro* drug release kinetics of INP18 formulation follows first order release with  $R^2$  value 0.990, and it follows Non-fickian type of diffusion with  $n$  value 0.727.

**Table 20: *In-Vitro* Release Kinetics of All Formulations from INP1 –INP18**

Formulation code	Zero order		First order		Higuchi		Krosmeier-Peppas		Drug release mechanism
	$r^2$	m	$r^2$	m	$r^2$	m	$r^2$	Diffusion Exponent (n)	
INP1	0.970	3.468	0.905	-0.042	0.908	17.48	0.926	0.604	NON-FICKIAN
INP2	0.965	2.146	0.982	-0.014	0.950	11.09	0.934	0.553	NON-FICKIAN
INP3	0.986	3.68	0.914	-0.043	0.868	17.99	0.918	0.761	NON-FICKIAN
INP4	0.991	2.58	0.994	-0.018	0.931	13.07	0.984	0.787	NON-FICKIAN
INP5	0.976	2.573	0.977	-0.019	0.944	13.18	0.969	0.615	NON-FICKIAN
INP 6	0.981	2.544	0.991	-0.010	0.949	13.04	0.990	0.721	NON-FICKIAN

INP7	0.990	2.792	0.993	-0.010	0.922	14.03	0.983	1.024	SUPER CASE-II
INP8	0.994	2.729	0.978	-0.020	0.914	13.63	0.974	0.744	NON-FICKIAN
INP9	0.992	2.612	0.992	-0.018	0.992	13.15	0.914	0.841	NON-FICKIAN
INP10	0.970	2.889	0.935	-0.022	0.815	13.79	0.860	0.824	NON-FICKIAN
INP11	0.971	2.807	0.968	-0.021	0.955	14.50	0.988	0.754	NON-FICKIAN
INP12	0.966	2.917	0.962	-0.022	0.844	14.31	0.973	0.865	NON-FICKIAN
INP13	0.968	2.751	0.987	-0.021	0.959	14.25	0.988	0.747	NON-FICKIAN
INP14	0.989	2.766	0.983	-0.020	0.935	14.0	0.996	0.796	NON-FICKIAN
INP15	0.980	3.403	0.938	-0.027	0.933	17.29	0.982	0.682	NON-FICKIAN
INP16	0.992	2.781	0.988	-0.011	0.933	14.05	0.999	0.816	NON-FICKIAN
INP17	0.994	2.441	0.976	-0.016	0.899	12.09	0.989	0.817	NON-FICKIAN
INP18	0.993	3.48	0.954	-0.027	0.932	17.61	0.984	0.727	NON-FICKIAN

## DISCUSSION

In this study, a series of preformulation and characterization studies were conducted on Imatinib mesylate to optimize its formulation as nanoparticles. The results obtained provide valuable insights into the physical and chemical properties of the drug, as well as its compatibility with various excipients. The characterization of the pure drug confirmed its identity as Imatinib mesylate. It appeared as a yellow powder and showed a melting point of 226.5°C, which is consistent with the reported range. Solubility studies demonstrated that Imatinib mesylate is soluble in pH 6.8 phosphate buffer, indicating its potential for formulation development using this medium. These findings are crucial as they confirm the drug's physical characteristics and solubility, which are key factors in formulating a stable and bioavailable product. Drug-excipient compatibility studies are essential to ensure that there are no interactions between the drug and the excipients used in the formulation. In this study, Fourier transform infrared spectroscopy (FTIR) was used to assess the possible incompatibilities between Imatinib mesylate and the excipients, such as ethyl cellulose and PVA. FTIR spectra were obtained for both Imatinib mesylate alone and in combination with the excipients. The spectra showed characteristic peaks corresponding to various functional groups in the drug and excipients. The absence of any significant changes in the peak positions or intensities indicated that there were no major interactions between the drug and the excipients, suggesting their compatibility for formulation development. This is crucial, as drug-excipient interactions can affect the stability, efficacy, and safety of the final dosage form. Differential scanning calorimetry (DSC) was performed to study the thermal behavior of Imatinib mesylate. DSC thermograms were obtained for both the pure drug and a physical mixture of the drug with the excipients. The DSC of the pure drug exhibited a peak at the melting point, confirming the purity of Imatinib mesylate. The DSC thermogram of the physical mixture showed peaks corresponding to the drug and the excipients, indicating their compatibility. The determination of  $\lambda_{\text{max}}$  (maximum absorbance wavelength) is crucial for the accurate analysis of drug concentrations in formulations using UV-visible spectrophotometry. In this study,  $\lambda_{\text{max}}$  for Imatinib mesylate in pH 6.8 phosphate buffer was determined to be 255 nm. This information allows for the precise quantification of the drug in further formulation and release studies. The calibration curve for Imatinib mesylate was constructed using different concentrations of the drug in the pH 6.8 phosphate buffer. The absorbance of the solutions was measured at 255 nm. The resulting

calibration curve showed a linear relationship between drug concentration and absorbance, with a high correlation coefficient ( $R^2$ ) of 0.997. This indicates that UV-visible spectrophotometry can be reliably used to quantitatively analyse Imatinib mesylate in formulations, ensuring accurate drug dosage in future experiments. The evaluation of formulation parameters is critical for assessing the quality and performance of nanoparticles. In this study, key parameters such as percentage yield, drug content, entrapment efficiency, particle size, zeta potential, and polydispersity index were evaluated. The percentage yield provides information about the efficiency of the nanoparticle preparation process. In this study, the percentage yield ranged from 57.2% to 99.3%. The observed variations in the percentage yield could be attributed to differences in formulation variables and processing methods. It is important to note that a higher percentage yield indicates a more efficient preparation process, resulting in a greater amount of the desired product. The drug content of the nanoparticles is a critical parameter to ensure accurate dosage delivery. In this study, the drug content ranged from 64.5% to 98.2%. Variations in drug content can arise from differences in formulation variables, drug-polymer interactions, and the efficiency of the encapsulation process. It is important to ensure that the drug content is within a specified range to deliver the desired therapeutic effect. The entrapment efficiency of nanoparticles is a key parameter that reflects the extent to which the drug is encapsulated within the polymer matrix. In this study, the entrapment efficiency ranged from 57.2% to 99.3%. Higher entrapment efficiency indicates a higher proportion of the drug being encapsulated and protected from degradation or premature release. The observed variations in entrapment efficiency can be attributed to the formulation variables, such as the drug-polymer ratio and the concentration of stabilizer. Particle size plays a crucial role in nanoparticle formulations as it affects their stability, drug release kinetics, and interaction with biological systems. In this study, the particle size ranged from 172.2 nm to 502.4 nm. The observed particle sizes are within the desired range for nanoparticles, indicating their suitability for further development. Zeta potential measurement provides valuable information about the surface charge of nanoparticles, which can influence their stability and interaction with biological systems. In this study, the zeta potential ranged from -26.2 mV to -3.43 mV, indicating that the nanoparticles had a negative surface charge. This negative charge can contribute to the stability of the nanoparticles and minimize their aggregation. It is important to note that zeta potential is influenced by the formulation variables and can be optimized to achieve the desired stability and performance of the nanoparticles. Polydispersity index (PDI) is used to evaluate the size distribution of nanoparticles. A PDI value of 1 indicates a monodisperse particle size distribution, while a higher value indicates a wider size distribution. In this study, all formulations had a PDI value of 1, indicating a narrow and monodisperse size distribution. This is desirable as it ensures uniformity in drug release and enhances the predictability of therapeutic effects. In-vitro drug release studies were performed to assess the drug release kinetics from the nanoparticles. These studies provide critical information about the release profiles of the drug from the formulation, which can influence the therapeutic efficacy and safety of the nanoparticles. The drug release profiles were evaluated at different time points, and the percentage cumulative drug release (%CDR) was calculated. The release kinetics were analyzed using various models, including zero-order, first-order, Higuchi, and Krosmeier-Peppas equations. The best-fit model was determined based on the highest correlation coefficient ( $R^2$ ) value and the best fit to the experimental data. The analysis of the in-vitro drug release studies revealed different release profiles for the formulations. The release profiles were characterized by an initial burst release followed by sustained release over a period of 24 hours. The release profiles can be attributed to various factors, including the drug-polymer ratio, concentration of stabilizer, and stirring speed. The optimized formulation (INP18) exhibited a sustained drug release profile, with 97.42% of the drug released over 24 hours. The release kinetics were analyzed using various mathematical models. The model that best fit the release data was determined based on the highest correlation coefficient ( $R^2$ ) value and the similarity between the predicted and observed data points. In this study, the release kinetics of the optimized formulation (INP18) followed first-order release kinetics, which is consistent with sustained release over time. The obtained release kinetics, including zero-order, first-order, Higuchi, and Krosmeier-Peppas, can provide valuable information about the mechanism and kinetics of drug release from the nanoparticles. The release mechanisms were classified as non-Fickian diffusion or



super case-II transport. These findings suggest that the drug release is controlled by a combination of diffusion and polymer erosion. The interpretation of the results obtained in this study provides valuable insights into the formulation and optimization of Imatinib mesylate nanoparticles. The characterization studies confirmed the identity of the drug and its compatibility with various excipients. The evaluation parameters demonstrated the quality and performance of the nanoparticles, including their drug content, entrapment efficiency, particle size, zeta potential, and release kinetics. These outcomes offer valuable information for the development of Imatinib mesylate nanoparticles as a drug delivery system.

## Conclusion

In summary, this study successfully formulated and evaluated Imatinib mesylate nanoparticles using the solvent evaporation method. The nanoparticles exhibited excellent characteristics, such as high entrapment efficiency, sustained drug release, and stable particle size and zeta potential. The optimized formulation demonstrated promising results with a controlled release mechanism. These findings suggest that the Imatinib mesylate nanoparticles could be a valuable drug delivery system with potential therapeutic benefits. Future research should focus on investigating the nanoparticles' in-vivo performance and in-vitro-in-vivo correlation (IVIVC) to better understand their behaviour in biological systems and their clinical applications.

## References

1. Deininger M, Buchdunger E, Druker BJ. The development of imatinib as a therapeutic agent for chronic myeloid leukemia. *Blood*. 2005 Apr 1;105(7):2640-53.
2. Druker BJ. Perspectives on the development of a molecularly targeted agent. *Cancer Cell*. 2002 Feb 1;1(1):31-6.
3. Druker BJ, Tamura S, Buchdunger E, Ohno S, Segal GM, Fanning S, Zimmermann J, Lydon NB. Effects of a selective inhibitor of the Abl tyrosine kinase on the growth of Bcr–Abl positive cells. *Nature medicine*. 1996 May 1;2(5):561-6.
4. Chen Y, Lu Y, Lee RJ, Xiang G. Nano encapsulated curcumin: and its potential for biomedical applications. *International Journal of Nanomedicine*. 2020 May 1;3099-120.
5. Bala I, Hariharan S, Kumar MR. PLGA nanoparticles in drug delivery: the state of the art. *Critical Reviews™ in Therapeutic Drug Carrier Systems*. 2004;21(5).
6. Pinto AC, Angelo S, Moreira JN, Simões S. Development, characterization, and in vitro evaluation of single or co-loaded imatinib mesylate liposomal formulations. *J Nanosci Nanotechnol*. 2012 Mar;12(3):2891-900. doi: 10.1166/jnn.2012.5703. PMID: 22755139.
7. Karimi M, Karimian K, Heli H. A nanoemulsion-based delivery system for imatinib and in vitro anticancer efficacy. *Brazilian Journal of Pharmaceutical Sciences*. 2021 Apr 26;56.
8. Bilia AR, Bergonzi MC, Boulos JC, Efferth T. Nanocarriers to enhance solubility, bioavailability, and efficacy of artemisinins. *World Journal of Traditional Chinese Medicine*. 2020 Jan 1;6(1):26-36.
9. Hoshyar N, Gray S, Han H, Bao G. The effect of nanoparticle size on in vivo pharmacokinetics and cellular interaction. *Nanomedicine (Lond)*. 2016 Mar;11(6):673-92. doi: 10.2217/nnm.16.5. Epub 2016 Mar 22. PMID: 27003448; PMCID: PMC5561790.
10. Sercombe L, Veerati T, Moheimani F, Wu SY, Sood AK, Hua S. Advances and challenges of liposome assisted drug delivery. *Frontiers in pharmacology*. 2015 Dec 1;6:286.
11. Kamaly N, Yameen B, Wu J, Farokhzad OC. Degradable controlled-release polymers, and polymeric nanoparticles: mechanisms of controlling drug release. *Chemical reviews*. 2016 Feb 24;116(4):2602-63.
12. Chadha R, Bhandari S. Drug–excipient compatibility screening—role of thermoanalytical and spectroscopic techniques. *Journal of pharmaceutical and biomedical analysis*. 2014 Jan 18;87:82-97.
13. Ranjit K, Baquee AA. Nanoparticle: an overview of preparation, characterization and application. *Int Res J Pharm*. 2013;4(4):47-57.

14. Wilczewska AZ, Niemirowicz K, Markiewicz KH, Car H. Nanoparticles as drug delivery systems. *Pharmacological reports*. 2012 Sep 1;64(5):1020-37.
15. Mohanraj VJ, Chen YJ. Nanoparticles-a review. *Tropical journal of pharmaceutical research*. 2006;5(1):561-73.
16. Fei CY, Salimon J, Said M. Optimisation of urea complexation by Box-Behnken design. *Sains Malaysiana*. 2010 Oct 1;39(5):795-803.